

Lefschetz Thimbles and Quantum Phases in Zero-Dimensional Bosonic Models

R Bharathkumar^{1,*} and Anosh Joseph^{1,†}

¹*Department of Physical Sciences, Indian Institute of Science Education and Research (IISER) Mohali, Knowledge City, Sector 81, SAS Nagar, Punjab 140306, India*

(Dated: June 25, 2022)

In this paper, by analyzing the underlying Lefschetz thimble structure, we study quantum phases in zero-dimensional scalar field theories with complex actions. Using first principles, we derive the Lefschetz thimble equations of these models, and discuss the issues when we apply the same calculations for more complicated systems. We also derive the conditional expressions involving relations among the parameters of the model, that would help us predict quantum phase transitions in these systems.

CONTENTS

I. Introduction	1
II. A Primer on Lefschetz Thimbles	2
III. Quartic Model with a Source Term	3
IV. Thimble Equations and Observables	4
A. Thimble Equations	4
B. Partition Function and Observables	5
V. Computing the Intersection Numbers	8
A. A Simple Demonstration using Airy Integral	8
B. In the Absence of the Source Term	9
1. Real Coupling	9
2. Complex Coupling	9
C. In the Presence of the Source Term	10
1. Real Source Parameter	10
2. Imaginary Source Parameter	10
D. In the Presence of \mathcal{PT} Symmetry	11
VI. Quantum Phase Transition and Change in Thimble Structure	12
VII. Summary of Results	15
VIII. Conclusions and Future Directions	15
Acknowledgments	16
A. Expressions for Boundaries of Phase Transitions	16
References	18

I. INTRODUCTION

We encounter path integrals with complex actions in many branches of physics. The prominent examples are the Minkowski path integral, Yang-Mills theory in the theta vacuum, Chern-Simons gauge theories, chiral gauge theories, and QCD with chemical potential. There are also quantum theories with complex actions that exhibit \mathcal{PT} symmetry [1–3]. It would be very useful to have a formalism that offers a promising tool to solve field theories containing complex path-integral weights.

A recently developing method to deal with quantum field theories with complex actions uses the complex analog of Morse theory from differential topology [4, 5]¹. There, the objects of primary interest, the so-called Lefschetz thimbles, are a set of sub-manifolds associated with a function that satisfy the Morse flow equation for the real part of the function. The central idea behind using this formalism is to recast the path integral in terms of a finite set of non-oscillatory integrals. Recent work on complex path integrals and connections to Lefschetz thimbles can be seen in Refs. [15–25]. In Refs. [26–31] the Lefschetz-thimble approach has been employed to study bosonic quantum field theories, and in Refs. [32–37] models including fermions were studied. The relevance of Lefschetz thimbles in the context of semi-classical expansion in asymptotically free quantum field theories is discussed in Refs. [38–42].

In this paper we explore the quantum phases in zero-dimensional scalar field theories with complex actions, containing quartic interactions and a source term. The Lefschetz thimble equations are derived, using first principles, in these models for various values of the coupling parameters. The set of conditions on the coupling parameters of the model can lead to discontinuities in the curve equations for thimbles. This in turn make the solutions simultaneously being either the thimble or the

¹ There exists another compelling method to deal with models containing complex actions. It is based on complex Langevin dynamics. See Refs. [6–14] for recent developments in using complex Langevin dynamics in quantum field theories with complex actions.

* r.bharathkumar@outlook.com

† anoshjoseph@iisermohali.ac.in

anti-thimble depending on the region in the complex plane under consideration. We refer to this interesting behavior as the ‘piecewise behavior’ of the solutions, since they appear themselves as piecewise thimbles/anti-thimbles/ghosts. Whether a thimble solution shows piecewise behavior or not depends on the set of coupling parameters of the model. We also derive the conditional expressions involving relations among the parameters of the model, that in turn, would help us predict quantum phase transitions in these systems. We also see that the underlying thimble structure undergoes a drastic change while the system is going through such a phase transition.

The paper is organized as follows. In Sec. II we provide a primer on Lefschetz thimbles by introducing the gradient flow equations of the given action. In Sec. III we introduce the model of our interest, a zero-dimensional bosonic model with complex action containing quartic interactions and a source term. The thimble equations for this model are derived next in Sec. IV. We discuss analytic expressions for the thimble and anti-thimble equations, and the ghost solutions. The model exhibits an interesting piecewise behavior for the thimbles and anti-thimbles when the parameters of the action take certain values. The partition function and observables of the model are also discussed. In Sec. V we discuss the phase transition boundaries starting with the Airy integral as a simple example. We discuss the boundaries of phase transitions for various combinations of the values of the coupling parameters. This includes the interesting case when the complex action exhibits \mathcal{PT} symmetry. We provide a few examples of phase transition boundaries in Sec. VI. We see that the structure of the thimbles undergoes a drastic change when the system goes through a quantum phase transition. In Sec. VII we provide a summary of the main results. In Sec. VIII we conclude and indicate possible future directions.

II. A PRIMER ON LEFSCHETZ THIMBLES

Intuitively, we can relate the Lefschetz thimbles to the original integration cycle of the quantum field theory in the following way. Let us denote the original integration cycle as $\mathcal{M}_{\mathbb{R}}$. We ‘complexify’ this manifold to $\mathcal{M}_{\mathbb{C}}$, that is, we take a complex manifold $\mathcal{M}_{\mathbb{C}}$ that contains the original manifold $\mathcal{M}_{\mathbb{R}}$ as a submanifold, with the requirement that the complex conjugate of an element of $\mathcal{M}_{\mathbb{R}}$ is the element itself. One can think of $\mathcal{M}_{\mathbb{R}} = \mathbb{R}^n$ and $\mathcal{M}_{\mathbb{C}} = \mathbb{C}^n$ for ease of understanding. An example more useful to gauge theories is $\mathcal{M}_{\mathbb{R}} = \text{SU}(n)$ and $\mathcal{M}_{\mathbb{C}} = \text{SL}(n, \mathbb{C})$, which is obtained by letting the field over which the Lie algebra of $\text{SU}(n)$ is defined to be \mathbb{C} instead of \mathbb{R} .

Post complexification, we identify the *Morse function* [43]. The Morse function in a loose sense determines these thimbles. A natural function to consider is the

action². Given a Morse function, we identify its *critical points* – points in $\mathcal{M}_{\mathbb{C}}$ where the Morse function is locally extremized. The next step, visually, can be thought of as continuously deforming $\mathcal{M}_{\mathbb{R}}$, the deformation being controlled by the Morse function through the Morse flow equations

$$\frac{dz^i}{dt} = g^{i\bar{j}} \frac{\partial \bar{S}}{\partial z^{\bar{j}}}, \quad \frac{d\bar{z}^{\bar{j}}}{dt} = g^{i\bar{j}} \frac{\partial S}{\partial z^i}, \quad (1)$$

where $g^{i\bar{j}}$ is the metric on $\mathcal{M}_{\mathbb{C}}$ and z_i are a set of local coordinates around the critical points of S . It can be checked immediately that the imaginary part of the action S is constant along the solution to the above equations.

As the final result of this construction, we obtain a pair of sub-manifolds, called the thimble and anti-thimble, associated with each critical point. The thimble is the ‘stable’ solution. That is, the action goes to infinity sufficiently rapidly along a thimble, so as to keep the integral involving $\exp(-S)$ to be convergent. The anti-thimble is the ‘unstable’ solution. An example familiar in physics is the method of steepest descent, and thus the Lefschetz thimbles formalism can be thought of as the generalization of the steepest descent method. A rigorous treatment of this construction can be found in Refs. [43–45].

An integral involving the action on the sub-manifold $\mathcal{M}_{\mathbb{R}}$ can now be written as a linear combination of integrals over the Lefschetz thimbles. In this language, the expression for the partition function associated with a system with action S is given as the weighted sum of contributions from the critical points ϕ_i of the action

$$Z = \sum_i n_i \int_{\mathcal{J}_i} D\phi e^{-S[\phi]}, \quad (2)$$

where the integral denotes integration over the Lefschetz thimble \mathcal{J}_i , which is associated with the i -th critical point ϕ_i of the action. The weight (also known as the intersection number) n_i is an integer that decides the contribution of a particular critical point to the partition function. Assuming that the critical points do not share a common gradient flow, given in Eq. (1), n_i is given by the number of times the anti-thimble intersects the original integration cycle \mathcal{M} [46]. That is,

$$n_i = \langle \mathcal{K}_i, \mathcal{M} \rangle. \quad (3)$$

An advantage of using Lefschetz thimbles is that on these thimbles, as discussed before, the imaginary part of the action remains constant. This is certainly a desirable property since, in the (Euclidean) path integral formalism of quantum field theories, the constant imaginary part of the action, $\text{Im}(S)$, in the integral, Eq. (2),

² The actual Morse function under consideration is the real part of $-S$ since by definition, Morse functions are real.

can be pulled out as a phase factor, and the remaining integral becomes a non-oscillatory integral³.

In zero spacetime dimensions the formalism simplifies greatly. For the majority of the situations considered in this work, the original integration cycle is the real line, \mathbb{R} . In this case, we end up dealing with curves in the plane of allowed degrees of freedom for the fields (i.e., \mathbb{C}) that satisfy the gradient flow equation

$$\frac{\partial \phi(t)}{\partial t} = -\overline{\left(\frac{\delta S}{\delta \phi}\right)}, \quad (4)$$

where t is a parameter and the overline represents complex conjugation. The thimble \mathcal{J}_i associated with the critical point ϕ_i of the action is defined as the solution to Eq. (4) that satisfies

$$\lim_{t \rightarrow \infty} \phi(t) = \phi_i,$$

and the anti-thimble \mathcal{K}_i satisfies

$$\lim_{t \rightarrow -\infty} \phi(t) = \phi_i.$$

By definition, the thimbles always end inside regions of stability⁴, while anti-thimbles end inside regions of instability.

III. QUARTIC MODEL WITH A SOURCE TERM

We are interested in the action, which is complex, with quartic interaction and source terms, in zero spacetime dimensions

$$S[\phi] = h\phi + \frac{\alpha}{2}\phi^2 + \frac{\beta}{4}\phi^4, \quad (5)$$

where h , α and β are complex coefficients. For convenience, we also express

$$\alpha = a + ib \quad \text{and} \quad \beta = c + id. \quad (6)$$

The motivation for considering this particular action is two-fold. First, the above action acts as an excellent toy model for understanding systems with complex actions, in the path integral formalism [48, 49], and how Lefschetz thimbles help mitigate the *sign problem*, while also being not too trivial and allowing us to showcase a

lot of rich dynamics that accompany the Lefschetz thimble analysis. Second, for the method employed in our calculations, quartic interactions are the highest, exactly solvable terms due to the Abel-Ruffini theorem in algebra [50–52] that states that there are no closed-form expressions for solutions to general polynomial equations of degree five or higher. Further, the inclusion of a source term ensures that we exhaust all physically possible situations for a system with quartic interactions.

The regions of stability (sometimes referred to as the Stokes wedges [53, 54]) are determined as follows. Since the integral in Eq. (2) involves the expression $\exp(-S)$, the integral is convergent in regions where, as ϕ approaches infinity, $\text{Re}(S[\phi]) \geq 0$. Since the highest order in our action is four, we get four wedges on the complex plane where the integral is convergent. This is shown schematically in Fig. 1.

One way to find the (anti-)thimble associated with a critical point is to solve the gradient flow equation, Eq. (4), for (anti-)thimbles. This, however, quickly becomes very complicated, even for simple forms of actions, due to the coupling between the real and imaginary parts of the differential equation. Instead, we exploit a very crucial property of (anti-)thimbles: the imaginary part of the action remains constant along these (anti-)thimbles. Therefore, to solve for the thimbles, we look for solutions to

$$\text{Im}(S[\phi] - S[\phi_i]) = 0. \quad (7)$$

We restrict our calculations to cases where h (the parameter controlling the linear term in the action) is small compared to α and β . We further restrict h to be either real or purely imaginary. This allows us to approximate the three critical points⁵ of the action as

$$\phi_0 = -\frac{h}{\alpha} + \mathcal{O}(h^3), \quad (8a)$$

$$\phi_{\pm} = \pm i\sqrt{\frac{\alpha}{\beta}} + \frac{h}{2\alpha} \pm i\frac{3h^2}{8}\sqrt{\frac{\beta}{\alpha^5}} + \mathcal{O}(h^3). \quad (8b)$$

The critical point ϕ_0 is close to the origin (that is, $\phi = 0$) for small h while the position of ϕ_{\pm} depends on the choice of the parameters. Let us denote the imaginary part of the action at a given critical point by ρ_i . That is,

$$\rho_i \equiv \text{Im}S[\phi_i], \quad i = -, 0, +. \quad (9)$$

For the particular action we are considering, they take the following forms

³ There is a possibility that the integral can pick up an oscillatory nature due to the Jacobian that transforms the integration measure. This, however, is much milder compared to the original integral and is referred to as the *mild sign problem* [47].

⁴ Regions of stability are defined as regions in the complex plane

where the integral in Eq. (2) remains convergent.

⁵ In our discussion here, the critical points are the points in the ϕ plane where the action gets extremized, as defined in Sec. I. They are not the points in the parameter space corresponding to phase transitions.

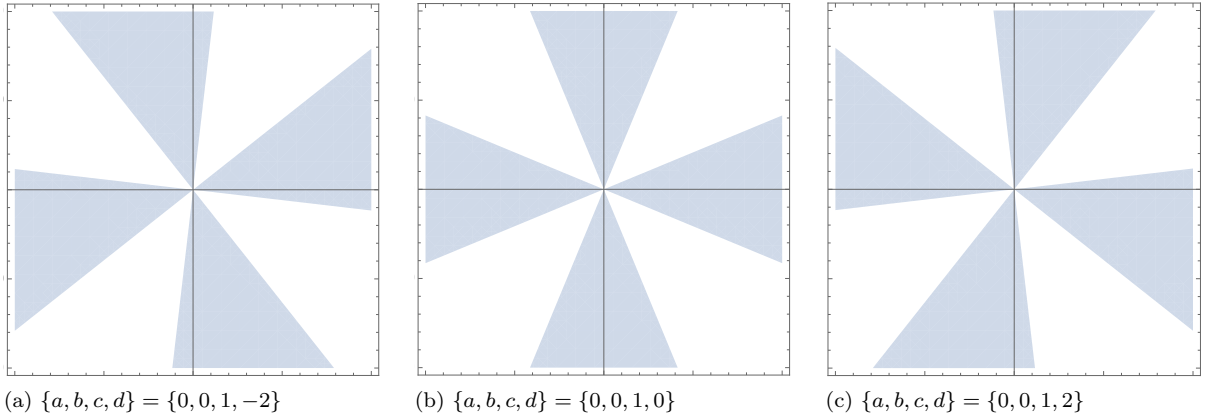


FIG. 1: (Color online). A schematic representation of the regions of stability at infinity for the action given in Eq. (5). Inside the shaded regions, the integral in Eq. (2) is convergent. In general, the position and shape of these wedges are controlled by the parameters h, α and β in the action.

$$\rho_0 = \left(\frac{b}{a^2 + b^2} \right) \text{Im}(h^2) + \mathcal{O}(h^3), \quad (10a)$$

$$\rho_{\pm} = \left[\frac{d(a^2 - b^2) - 2abc}{4(c^2 + d^2)} \right] \pm \text{Im} \left(ih \sqrt{\frac{(ac + bd) + i(bc - ad)}{c^2 + d^2}} \right) - \frac{b}{4(a^2 + b^2)} \text{Im}(h^2) + \mathcal{O}(h^3). \quad (10b)$$

We note that the convergence of the partition function integral given in Eq. (2) requires the real part c of β to be positive when the original integration cycle is \mathbb{R} . However, when c is negative, which is the case when the action possesses \mathcal{PT} symmetry (which we will see later), the standard procedure is to take an integration cycle about the angles $5\pi/4$ and $7\pi/4$ in the complex plane (that is, in the third and the fourth quadrant, respectively) [55, 56]. This choice ensures that the partition function integral remains convergent.

Parametrizing the field as

$$\phi = x + iy,$$

this amounts to choosing our integration cycle in the cases where c is negative, as

$$y(x) = \begin{cases} x & \text{for } x \leq 0, \\ -x & \text{for } x > 0. \end{cases} \quad (11)$$

IV. THIMBLE EQUATIONS AND OBSERVABLES

A. Thimble Equations

As discussed in Sec. III, we solve for the (anti-)thimble by equating the imaginary part of the action at a generic value of ϕ to the imaginary part of the action at one of its critical points. The equation for the (anti-)thimble corresponding to ϕ_0 when $h = 0$ and $d = 0$ was derived

by Aarts in Ref. [57]. We recreate those results here as a primer, and for completeness.

Substituting ρ_0 into the constraint given in Eq. (7), having set $h = 0$ and $d = 0$, we obtain the constraint

$$-cxy^3 - \frac{b}{2}y^2 + (ax + cx^3)y + \frac{b}{2}x^2 = 0. \quad (12)$$

Solving for y as a function of x , we obtain the thimble and anti-thimble, \mathcal{J}_0 and \mathcal{K}_0 , respectively, associated with the critical point ϕ_0

$$y(x) = \frac{1}{6cx} \left(-b + e^{-i\theta} \frac{\Delta_2}{\Delta_1} + e^{i\theta} \Delta_1 \right), \quad (13a)$$

$$\Delta_1 = \left(b\Delta_3 + \sqrt{b^2\Delta_3^2 - \Delta_2^3} \right)^{1/3}, \quad (13b)$$

$$\Delta_2 = b^2 + 12cx^2(a + cx^2), \quad (13c)$$

$$\Delta_3 = b^2 + 18cx^2(a - 2cx^2). \quad (13d)$$

Here $\theta \in \{-\frac{\pi}{3}, 0, \frac{\pi}{3}\}$. In Fig. 2 we show the three curves corresponding to the three values of the parameter θ . The thimble corresponds to $\theta = -\frac{\pi}{3}$ and the anti-thimble corresponds to $\theta = \frac{\pi}{3}$. The curves for $\theta = 0$ are paths of constant $\text{Im} S$ that are neither thimbles nor anti-thimbles. We shall refer to these curves as the *ghost solutions* or *ghosts*.

Similarly, when solving for ϕ_{\pm} , we obtain Eq. (13), but with Eq. (13d) now changed to the following form

$$\Delta_3 = b^2 + 72cx^2(a - cx^2). \quad (14)$$

In this case, $\theta = 0$ corresponds to the thimbles for both ϕ_+ and ϕ_- . The curve has two branches, one for $x < 0$ and the other for $x > 0$. The anti-thimble associated with ϕ_+ has $\theta = -\frac{\pi}{3}$. The anti-thimble associated with ϕ_- has $\theta = \frac{\pi}{3}$. In Fig. 2 we show the thimbles, anti-thimbles and ghosts for all the critical points, ϕ_0 and ϕ_{\pm} , of the action for the parameters $a = 1$, $b = 1$, $c = 1$, $d = 0$, and $h = 0$.

So far we have restricted the model to the case where $h = 0$ and $d = 0$. Let us now do away with the restriction on d while still maintaining the constraint $h = 0$. The thimble equation given in Eq. (12) is now modified as

$$\frac{d}{4}y^4 - cxy^3 - \left(\frac{b}{2} + \frac{3d}{2}x^2\right)y^2 + (ax + cx^3)y + \frac{b}{2}x^2 + \frac{d}{4}x^4 = \rho_i. \quad (15)$$

Rearranging the above equation in the form

$$Ay^4 + By^3 + Cy^2 + Dy + E = 0,$$

we obtain the equation of curves, $y_k(x)$, $k = 1, 2, 3, 4$, for (anti-)thimbles as a function of x

$$y_{1,2} = -\frac{B}{4A} - S \pm \frac{1}{2}\sqrt{-4S^2 - 2P + \frac{Q}{S}}, \quad (16a)$$

$$y_{3,4} = -\frac{B}{4A} + S \pm \frac{1}{2}\sqrt{-4S^2 - 2P - \frac{Q}{S}}, \quad (16b)$$

$$P = \frac{8AC - 3B^2}{8A^2}, \quad (16c)$$

$$Q = \frac{B^3 - 4ABC + 8A^2D}{8A^3}, \quad (16d)$$

$$R = \left(\frac{\Delta_1 + \sqrt{\Delta_1^2 - 4\Delta_0^3}}{2}\right), \quad (16e)$$

$$S = \frac{1}{2}\sqrt{-\frac{2}{3}P + \frac{1}{3a}\left(R + \frac{\Delta_0}{R}\right)}, \quad (16f)$$

$$\Delta_0 = C^2 - 3BD + 12AE, \quad (16g)$$

$$\Delta_1 = 2C^3 - 9BCD + 27B^2E + 27AD^2 - 72ACE. \quad (16h)$$

Although the solutions to the thimble equation given in Eq. (15) exist in the form of Eq. (16), there are a few caveats we would like to stress on. There are too many conditions⁶ to keep track of due to the requirement that $x, y \in \mathbb{R}$. These conditions could potentially lead to discontinuities in the curve equations, $y_k(x)$, $k = 1, 2, 3, 4$, for the thimbles in Eq. (16). Further, the requirement of keeping track of these conditions manifests itself as the four solutions simultaneously being either the thimble or the anti-thimble depending on the region in the complex plane under consideration. We will refer to this as the

‘piecewise behavior’ of the solutions since they appear themselves as piecewise thimbles/anti-thimbles/ghosts. Whether a solution shows piecewise behavior or not depends on the set of parameters $\{a, b, c, d\}$.

Let us consider the examples illustrated in Figs. 3 and 4. We see that the solution y_1 for ϕ_0 gives the thimble for $x < 0$ and a ghost for $x > 0$, y_2 gives the anti-thimble for $x < 0$ and a ghost for $x > 0$, y_3 gives the anti-thimble for $x > 0$ and a ghost for $x < 0$, and y_4 for gives the anti-thimble for $x > 0$ and a ghost for $x < 0$. Similarly, for ϕ_{\pm} , the solutions y_1 and y_2 give the thimble for both $x < 0$ and $x > 0$, and y_3 and y_4 give the thimble for both $x < 0$ and $x > 0$. However, they still exhibit the piecewise behavior. There definitely are parameter sets $\{a, b, c, d\}$ for which the piecewise behavior might not be exhibited. One such case is when $a = 1$, $b = 1$, $c = 1$, and $d = 1$; six of the eight solutions do not exhibit this behavior. (We show this in Figs. 5 and 6.) These cases, however, seem to be exceptions rather than the norm.

From the thimble/anti-thimble/ghost solutions given in Eq. (16), we see that obtaining the curves for the case $h \neq 0$ is straightforward. If h is real, then C changes from $(ax + cx^3)$ to $(h + ax + cx^3)$ while E remains the same, except for the change in ρ_i . If h is purely imaginary, then C remains unchanged and E gains an additional hx term apart from the change to ρ_i . This situation also suffers from the issues discussed earlier for the case where h was taken to zero while d was non-zero.

B. Partition Function and Observables

Let us consider the action given in Eq. (5) for the case $h = 0$ (the so-called quartic model)

$$S[\phi] = \frac{\alpha}{2}\phi^2 + \frac{\beta}{4}\phi^4. \quad (17)$$

We can construct an n -point function the following way

$$\langle \phi^n \rangle = \frac{1}{Z} \int D\phi \phi^n e^{-S[\phi]}, \quad Z = \int D\phi e^{-S[\phi]}. \quad (18)$$

Consider the following integral associated with the above action along the original integration cycle \mathbb{R}

$$I_n = \int_{-\infty}^{\infty} dx x^n e^{-\left(\frac{\alpha}{2}x^2 + \frac{\beta}{4}x^4\right)}. \quad (19)$$

Since the integrand is of odd parity under the exchange $x \rightarrow -x$ when n is odd, the above integral is non-zero only for even values of n . The partition function is recovered when $n = 0$, and the observables for the system are related to the above integral as

$$\langle \phi^n \rangle = \frac{1}{Z} I_n. \quad (20)$$

The exact result of the integral is known in terms of modified Bessel functions for the cases $n = 0$ and $n = 2$,

⁶ A visual summary of these conditions can be found in Ref. [58]

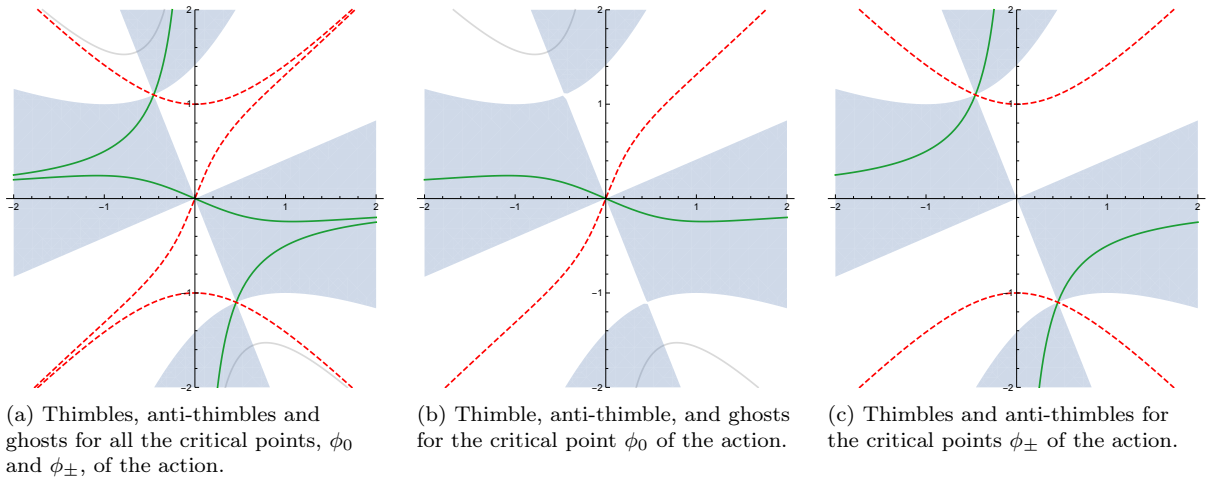


FIG. 2: (Color online). The solutions to the thimble equation given in Eq. (7), corresponding to the critical points ϕ_0 and ϕ_{\pm} , for the parameters $a = 1$, $b = 1$, $c = 1$, $d = 0$, and $h = 0$. In all the three figures, the green solid curves represent the thimbles, red dashed curves represent the anti-thimbles, and the grey solid curves represent the ghosts. The shaded regions represent the regions where $\text{Re}(S) \geq 0$.

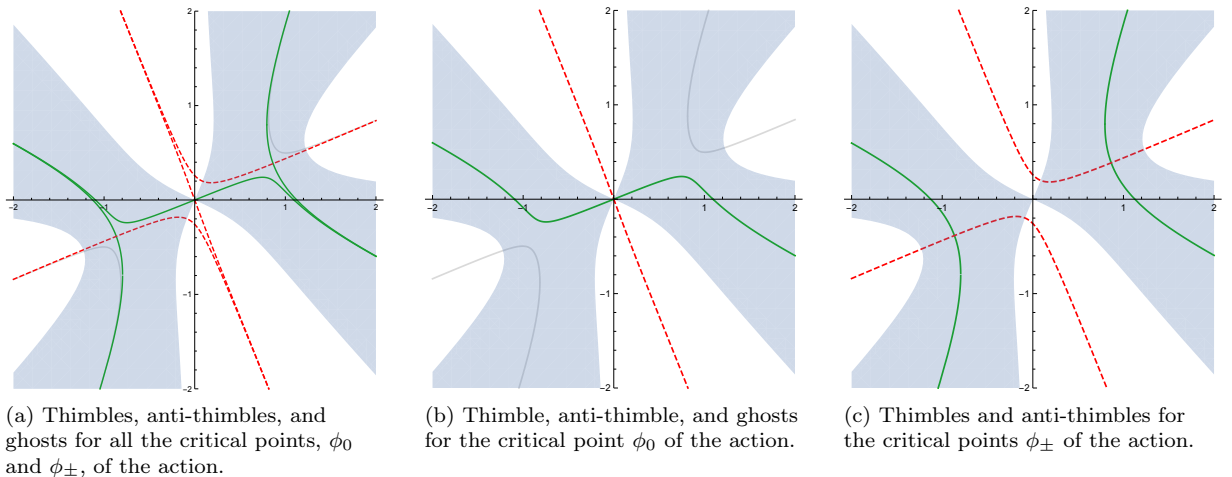


FIG. 3: (Color online). The solutions to the thimble equation given in Eq. (7), corresponding to the critical points ϕ_0 and ϕ_{\pm} , for the parameters $a = 1$, $b = -0.9$, $c = 0$, $d = 1.5$, and $h = 0$. In all the three figures, the green solid curves represent the thimbles, red dashed curves represent the anti-thimbles, and the grey solid curves represent the ghosts. The shaded regions represent the regions where $\text{Re}(S) \geq 0$.

for $\text{Re}(\alpha) > 0$ and $\text{Re}(\beta) > 0$, as [59]

$$Z = \sqrt{\frac{\alpha}{2\beta}} e^{\alpha^2/(8\beta)} K_{1/4}\left(\frac{\alpha^2}{8\beta}\right), \quad (21)$$

$$\langle \phi^2 \rangle = \frac{\alpha}{4\beta} \frac{K_{-3/4}\left(\frac{\alpha^2}{8\beta}\right) + K_{5/4}\left(\frac{\alpha^2}{8\beta}\right)}{K_{1/4}\left(\frac{\alpha^2}{8\beta}\right)} - \frac{\alpha}{2\beta} - \frac{1}{\alpha}. \quad (22)$$

Here K is the modified Bessel function of the second kind. In the case where $\text{Re}(\alpha) < 0$, we replace K in Z with I , the modified Bessel function of the first kind.

Integrating Eq. (19) by parts, rearranging, and dividing by Z , we obtain a recursion relation for observables

of the theory

$$(2n+1)\langle \phi^{2n} \rangle - \alpha \langle \phi^{2(n+1)} \rangle - \beta \langle \phi^{2(n+2)} \rangle = 0. \quad (23)$$

Thus, since the closed-form expressions for the partition function and the observable $\langle \phi^2 \rangle$ are known, all observables of the theory are known and can be written in terms of the two using Eq. (23). The relation could potentially be used to determine the partition function of the action with sources. The partition function is given

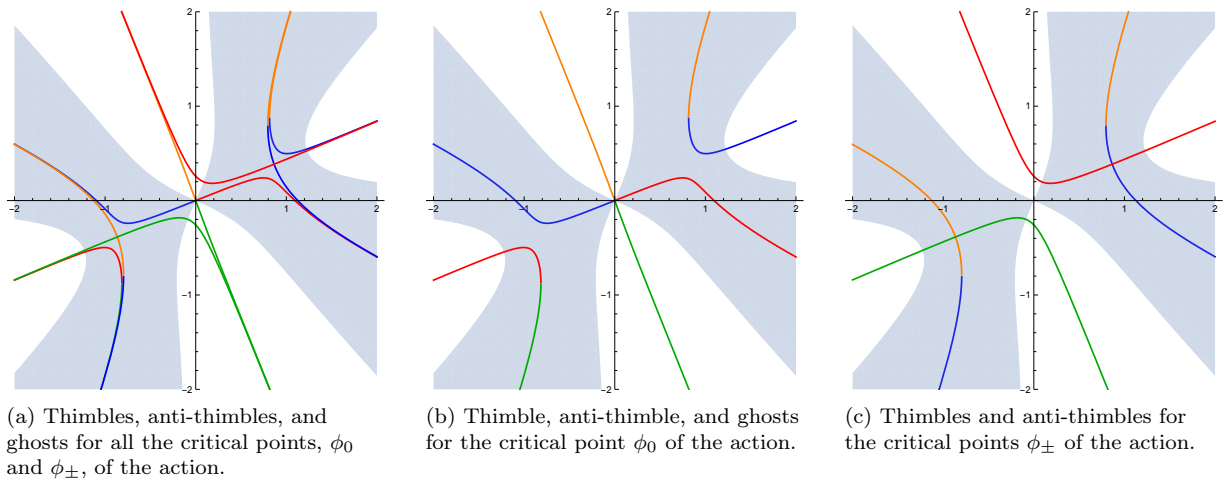


FIG. 4: (Colour online). Demonstration of the piecewise behavior by the solutions to the thimble equation given in Eq. (7), corresponding to the critical points ϕ_0 and ϕ_{\pm} of the action, for the parameters $a = 1$, $b = -0.9$, $c = 0$, $d = 1.5$, and $h = 0$. In all the three figures, the blue solid curves correspond to solution y_1 , orange solid curves to the solution y_2 , green solid curves to the solution y_3 and the red solid curve to the solution y_4 . The shaded regions denote the regions where $\text{Re}(S) \geq 0$.

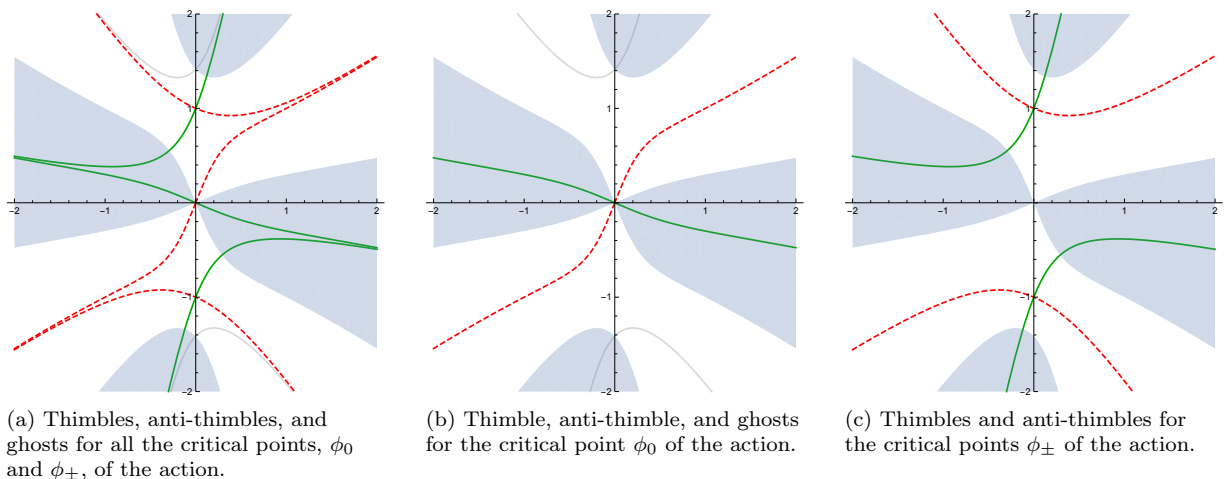


FIG. 5: (Colour online). The solutions to the thimble equation, Eq. (15), corresponding to ϕ_0 (Middle) and ϕ_{\pm} (Right), for the parameters $a = 1$, $b = 1$, $c = 1$, $d = 1$, and $h = 0$. In all the three figures, the green solid curves represent the thimbles, red dashed curves represent the anti-thimbles, and the grey solid curves represent the ghosts. The shaded regions represent the regions where $\text{Re}(S) \geq 0$.

by

$$\begin{aligned} Z_{\text{sources}} &= \int_{-\infty}^{\infty} dx e^{-(hx + \frac{\alpha}{2}x^2 + \frac{\beta}{4}x^4)}, \\ &= \int_{-\infty}^{\infty} dx e^{-hx} e^{-(\frac{\alpha}{2}x^2 + \frac{\beta}{4}x^4)}. \end{aligned} \quad (24)$$

Taylor expanding the first exponential, we get

$$Z_{\text{sources}} = \sum_{n=0}^{\infty} \frac{h^{2n}}{(2n)!} I_{2n}, \quad (25)$$

and from the recurrence relation derived above, Z_{sources} can be written solely in terms of I_0 and I_2 . However, this is not valid, as will be shown in Sec. VI, due to a very subtle change in the behavior of the critical points away from the origin (that is, the critical points ϕ_+ and ϕ_-).

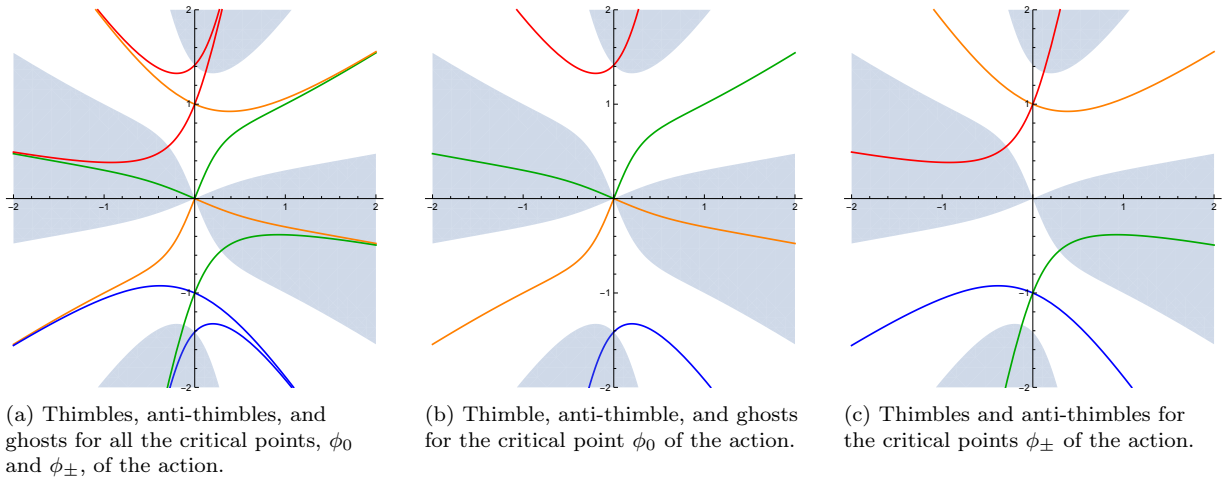


FIG. 6: (Colour online). Demonstration of piecewise behavior by the thimble solutions to Eq. (7), corresponding to ϕ_0 and ϕ_{\pm} , for the parameters $a = 1$, $b = 1$, $c = 1$, $d = 1$, and $h = 0$. In all the three figures, the blue solid curves corresponds to solution y_1 , orange solid curves to solution y_2 , green solid curves to solution y_3 and red solid curves to solution y_4 . The shaded regions denote the regions where $\text{Re}(S) \geq 0$.

V. COMPUTING THE INTERSECTION NUMBERS

The intersection number n_i , defined in Eqs. (2) and (3), being an integer, greatly controls the behavior of the partition function and observables of the model. As the parameters of the action are changed, the intersection number corresponding to a critical point could potentially change, which results in an abrupt change in the value of the partition function, and as a result, an abrupt change in the values of the observables of the system. The most dramatic among these is the case when the intersection number takes the value zero, and this in turn results in the corresponding critical point not contributing to the dynamics of the system. This change in the intersection number is referred by the name *Stokes phenomena*⁷ [4, 62] and this phenomenon points at quantum phase transitions in the system.

Despite having a few issues as discussed in Sec. IV, the power of using Eq. (7) to solve for (anti-)thimbles is the fact that it captures the information about these intersection numbers. Using this, we can look for the values of the parameters around which the intersection number changes, and thus allowing us to predict the boundaries of phase transitions.

One of our main results will be the analytic expressions for the combined intersection number of thimbles and

anti-thimbles of the zero-dimensional scalar field theory, with quartic interactions and a source term.

To arrive at these expressions, for the cases where c is positive, we use the fact that the original integration cycle \mathbb{R} corresponds to $y = 0$. Substituting this in Eq. (7), we obtain a polynomial equation in x of degree four or lower. Looking at the number of real solutions to the polynomial equation (remember, $x \in \mathbb{R}$) gives us the information about the number of times the thimbles and anti-thimbles⁸ intersect the original integration cycle. When we look at the action with \mathcal{PT} symmetry, we substitute Eq. (11) in Eq. (7) and repeat the analysis.

A. A Simple Demonstration using Airy Integral

Before we present our results for the action Eq. (5), we demonstrate quantum phase transitions in the Airy integral as a primer.

Consider the following integral

$$\text{Ai}(\lambda) = \int_{-\infty}^{\infty} \exp\left(i\left\{\frac{x^3}{3} + \lambda x\right\}\right), \quad (26)$$

⁷ An alternative, and equivalent, definition used frequently in the literature in the context of integration by the method of steepest descent is the change in the asymptotic formula for the same analytic function when the parameters of the function are changed [60, 61].

⁸ The number of solutions could potentially also contain information about the number of times a ghost solution intersects the original integration cycle. However, we have not come across a situation where a ghost solution intersects the real line. This is explained by the observation that a ghost solution always has one end inside the region of stability and the other end inside the region of instability. This, along with the fact that these curves do not intersect either the thimble or the anti-thimble of the same critical point tells us that the ghosts are always away from the real line.

where we restrict λ to take real values. The integral in Eq. (26) is equivalent to taking our action (after continuation to the complex plane) as

$$S[\phi] = -i \left\{ \frac{\phi^3}{3} + \lambda\phi \right\}. \quad (27)$$

There are two critical points of this action, namely

$$\phi_{\pm} = \pm i\sqrt{\lambda}. \quad (28)$$

At these critical points, the action takes the values

$$S[\phi_{\pm}] = \pm \frac{2}{3}\lambda^{3/2}. \quad (29)$$

Using our previous notation for ϕ as $\phi = x + iy$, the imaginary part of the action is

$$\text{Im}(S[\phi]) = \frac{3xy^2 - x^3}{3} - \lambda x. \quad (30)$$

To look for phase transition boundaries, we look for the number of real solutions to the equation

$$\text{Im}(S[\phi])|_{\text{along } \mathbb{R}} = \text{Im}S[\phi_{\pm}], \quad (31)$$

which is equivalent to putting $y = 0$ in Eq. (7). Thus we look for real solutions to the equation

$$\frac{-x^3}{3} - \lambda x = 0. \quad (32)$$

For cubic equations, the number of solutions depends only on the sign of the discriminant, which for the above equation is

$$\Delta = -\frac{4}{3}\lambda. \quad (33)$$

When the discriminant is negative, the number of real solutions to the cubic equation is one, and when the discriminant is positive, the number of solutions is three. Thus we expect a phase transition at $\lambda = 0$. In fact, this phase transition coincides with the change in the asymptotic expansion of $\text{Ai}(\lambda)$.

There is a very subtle detail that must be noted. For real λ , it is not possible to find the thimble for ϕ_- and the anti-thimble for ϕ_+ without deforming λ into the complex plane as $\lambda + i\epsilon$ for small ϵ . This occurs because when λ is real, the two critical points are always connected by a *Stokes ray*. More specific to our method, this problem arises because when λ is real, Eq. (31) has the RHS = 0. This leads to four curves being described by a polynomial equation of degree three, which cannot occur unless the critical points are connected by a flow. This is referred to as being connected by a Stokes ray [4]. The deformation $\lambda \rightarrow \lambda + i\epsilon$ moves the critical points away from the Stokes ray, allowing us to find the thimbles and anti-thimbles.

We can further complicate this case and take λ in Eq. (26) to be complex. This shows a similar phase transition structure, where the phase boundary is $|\arg(x)| = 2\pi/3$,

and was shown explicitly using the Lefschetz thimbles formalism in Ref. [46].

We now move on to our action with quartic interactions. Due to the differences in algebraic calculations and physical interpretations, we divide our results into multiple cases, and provide the detailed calculations that led to the results separately in Appendix A.

B. In the Absence of the Source Term

1. Real Coupling

We begin with the case where the parameters satisfy $h = 0$, $\alpha, \beta \in \mathbb{C}$, $\text{Re}(\beta) \geq 0$, and $d = 0$. The thimble equation, Eq. (7), gives a quadratic in x , from which the intersection numbers can trivially be found based on the conditions given below

$$n_i \begin{cases} = 1 & \text{when } i = 0, \forall \alpha, \beta, \\ \leq 1 & \text{when } i = \pm, \frac{a}{c} < 0, \\ = 0 & \text{when } i = \pm, \frac{a}{c} > 0. \end{cases} \quad (34)$$

This is the easiest of the cases that have been considered. In further analyses, the possibility of $d = 0$, where the equations reduce to a quadratic instead of the original quartic in x , is not considered since repeating the calculation by requiring $d = 0$ is straightforward.

2. Complex Coupling

Upon relaxing the condition on d while maintaining $h = 0$, $\alpha, \beta \in \mathbb{C}$, and $\text{Re}(\beta) \geq 0$, the polynomial obtained from Eq. (7) is a bi-quadratic in x .

Let us define the variables Δ , Π and Σ , which are related to the discriminant, product of roots, and sum of roots, respectively as outlined in Appendix A, as

$$\Delta = \frac{(bc - ad)^2}{(c^2 + d^2)}, \quad (35a)$$

$$\Pi = \frac{d(b^2 - a^2) + 2abc}{d(c^2 + d^2)}, \quad (35b)$$

$$\Sigma = \frac{b}{d}. \quad (35c)$$

Then the intersection number for the critical point ϕ_0 is determined using the conditions in Table I, and the intersection number for the critical points ϕ_{\pm} is determined using the conditions in Table II.

There are two comments to be made about these results. First, in both the Tables I and II (and later), we have extensively used the fact that (anti-)thimbles pass through the corresponding critical points. Further, in the situations discussed in this section, the (anti-)thimbles are not connected by the same flow equation, except for points in the parameter space at which the intersection

Condition	Intersection number
$\Sigma < 0$	≤ 3
$\Sigma \geq 0$	$= 1$

TABLE I: Constraints on the intersection number for the critical point ϕ_0 when $h = 0$, $\alpha, \beta \in \mathbb{C}$, $\text{Re}(\beta) \geq 0$, and $d \neq 0$.

number changes. Thus we have also used the fact that a (anti-)thimble of a particular critical point does not pass through any other critical point. Second, if a condition given in these tables does not provide any condition for a specific relation between the parameters (for instance, Π and Δ in Table I), it is to be understood that the value of that particular relation does not affect the intersection number.

Condition	Intersection number
$\Delta > 0, \Pi > 0, \Sigma < 0$	≤ 4
$\Delta > 0, \Pi = 0, \Sigma < 0$	≤ 2
$\Delta > 0, \Pi < 0$	≤ 2
$\Delta = 0, \Sigma < 0$	≤ 2
$\Delta > 0, \Pi > 0, \Sigma \geq 0$	$= 0$
$\Delta > 0, \Pi = 0, \Sigma \geq 0$	$= 0$
$\Delta = 0, \Sigma \geq 0$	$= 0$

TABLE II: Constraints on the intersection number for the critical points ϕ_{\pm} when $h = 0$, $\alpha, \beta \in \mathbb{C}$, $\text{Re}(\beta) \geq 0$, and $d \neq 0$.

As an illustration, let us determine the boundary at which the Stokes phenomena occurs for the choice of constants $a = 1$, $c = 0$, and $d = 1.5$, as derived by Fukushima and Tanizaki in Ref. [62]⁹. Conditions for Π given in Table II imply that all three thimbles to contribute when $b \in (-\infty, -1) \cup (1, \infty)$. Conditions for Σ in Tables I and II further require $b < 0$, which implies that when $b \in (-\infty, -1)$, all three thimbles contribute, and that Stokes phenomena is observed around $b = -1$.

C. In the Presence of the Source Term

1. Real Source Parameter

We now relax the condition on h to $h \in \mathbb{R}$. The obtained equation, like the previous case, is a bi-quadratic but with a change to the part independent of x .

Again let us introduce the variables Δ , Π and Σ as

$$\Delta = b^2 + 4d\rho_i, \quad (36)$$

$$\Pi = \frac{\rho_i}{d}, \quad (37)$$

$$\Sigma = \frac{b}{d}. \quad (38)$$

Here ρ_i is the imaginary part of the action, as defined in Eq. (10). The intersection number for each critical point ϕ_i is now determined by the conditions given in Table III.

Condition	Intersection number
$\Delta > 0, \Pi > 0, \Sigma < 0$	≤ 4
$\Delta > 0, \Pi = 0, \Sigma < 0$	≤ 3
$\Delta > 0, \Pi < 0$	≤ 2
$\Delta = 0, \Sigma < 0$	≤ 2
$\Delta > 0, \Pi = 0, \Sigma > 0$	≤ 1
$\Delta = 0, \Sigma = 0$	≤ 1
$\Delta > 0, \Pi > 0, \Sigma > 0$	$= 0$
$\Delta = 0, \Sigma > 0$	$= 0$
$\Delta < 0$	$= 0$

TABLE III: Constraints on the intersection number for the critical points ϕ_0, ϕ_{\pm} when $h \neq 0$, $h \in \mathbb{R}$, $\alpha, \beta \in \mathbb{C}$, $\text{Re}(\beta) \geq 0$, and $d \neq 0$.

For the situation where $\Delta > 0$, $\Pi \geq 0$, $\Sigma = 0$, the intersection number depends on the critical point under question. For ϕ_0 , the intersection number will be equal to one, while for ϕ_{\pm} , the intersection number is zero.

2. Imaginary Source Parameter

Let us consider the case when the source parameter is purely imaginary. Defining

$$\Delta = -\frac{1}{16} (64d^3\rho_i^3 + 32b^2d^2\rho_i^2 + 72bd^2h^2\rho_i + 27d^2h^4 + 4b^4d\rho_i + 2b^3dh^2), \quad (39)$$

$$\Delta_0 = \frac{1}{4} (b^2 - 12d\rho_i), \quad (40)$$

$$P = bd, \quad (41)$$

$$Q = -\frac{1}{4} (4d\rho_i + b^2d^2), \quad (42)$$

$$R = \frac{d^2h}{2}, \quad (43)$$

we obtain the conditions on the intersection number. They are provided in Table IV.

⁹ Note that the convention for constants used in Ref. [62] is slightly different but nonetheless, the results remain the same.

Condition	Intersection number
$\Delta > 0, P < 0, Q < 0$	≤ 4
$\Delta = 0, P < 0, Q < 0, \Delta_0 \neq 0$	≤ 3
$\Delta = 0, \Delta_0 = 0, Q \neq 0$	≤ 2
$\Delta = 0, Q = 0, P < 0$	≤ 2
$\Delta < 0$	≤ 2
$\Delta = 0, Q > 0$	≤ 1
$\Delta = 0, P > 0$	≤ 1
(given $Q \neq 0$ or $R \neq 0$)	
$\Delta = 0, \Delta_0 = 0, Q = 0$	≤ 1
$\Delta > 0, P > 0, Q > 0$	$= 0$
$\Delta = 0, P > 0, Q = 0, R = 0$	$= 0$

TABLE IV: Constraints on the intersection number for ϕ_0, ϕ_{\pm} when $h \in \mathbb{C}, \text{Re}(h) = 0, \alpha, \beta \in \mathbb{C}, \text{Re}(\beta) \geq 0$, and $d \neq 0$.

D. In the Presence of \mathcal{PT} Symmetry

We now specialize to actions that possess so-called \mathcal{PT} -symmetry, where \mathcal{P} is the parity symmetry and \mathcal{T} is the time reversal invariance. In zero dimensions, any real function of ix is symmetric under \mathcal{PT} transformation [55]. That is, our action should be of the form¹⁰

$$S = \sum_n -a_n(ix)^n, \quad (44)$$

with n denoting integers and a_n representing real numbers.

Comparing Eq. (44) with Eq. (5), we see that Eq. (44) corresponds to the case with $h \in \mathbb{C}, \text{Re}(h) = 0$, and $\alpha = a, \beta = c \in \mathbb{R}$, such that $c < 0$. This is equivalent to replacing $h \rightarrow ih$ and $c \rightarrow -c$ in Eqs. (5), (8) and (10), and maintaining $h \in \mathbb{R}, c > 0$. This leads to

$$\phi_0 = -\frac{ih}{a} + \mathcal{O}(h^3), \quad (45a)$$

$$\phi_{\pm} = \pm\sqrt{\frac{a}{c}} - \frac{ih}{2a} \pm \frac{3h^2}{8}\sqrt{\frac{c}{a^5}} + \mathcal{O}(h^3). \quad (45b)$$

The values of ρ_i depend on the value of a .

$$\rho_i = \begin{cases} 0 & \text{when } a \leq 0, \forall i, \\ 0 & \text{when } a > 0, i = 0, \\ +h\sqrt{\frac{a}{|c|}} & \text{when } a > 0, i = +, \\ -h\sqrt{\frac{a}{|c|}} & \text{when } a > 0, i = -. \end{cases} \quad (46)$$

We first explore the case where a is positive. In this situation we obtain a set of quadratic equations. Solving for each sector in Eq. (11), and combining the results,

we obtain the conditions in Tables V and VI, where we have defined

$$\Delta_R = h^2 + 4a\rho_i, \quad (47)$$

$$\Delta_L = h^2 - 4a\rho_i, \quad (48)$$

$$\Sigma = \frac{h}{a}, \quad (49)$$

$$\Pi = \frac{\rho}{a}. \quad (50)$$

Combining the intersection numbers for each sector is highly non-trivial, and more information on how they were combined can be found in Appendix A.

Condition	Intersection number
$\Sigma > 0$	≤ 3
$\Sigma < 0$	≤ 1

TABLE V: Constraints on the intersection number for the critical point ϕ_0 when the action is \mathcal{PT} -symmetric.

Condition	Intersection number
$\Delta_R > 0, \Delta_L > 0, \Sigma > 0$	≤ 3
$\Delta_R = 0, \Delta_L > 0, \Sigma > 0, \Pi < 0$	≤ 2
$\Delta_R > 0, \Delta_L = 0, \Sigma > 0, \Pi > 0$	≤ 2
$\Delta_R < 0, \Delta_L > 0, \Sigma > 0, \Pi > 0$	≤ 2
$\Delta_R > 0, \Delta_L < 0, \Sigma > 0, \Pi < 0$	≤ 2
$\Delta_R = 0, \Delta_L < 0, \Sigma > 0$	≤ 1
$\Delta_R > 0, \Delta_L < 0, \Pi > 0$	≤ 1
$\Delta_R > 0, \Delta_L = 0, \Sigma < 0, \Pi > 0$	≤ 1
$\Delta_R > 0, \Delta_L > 0, \Sigma < 0, \Pi > 0$	≤ 1
$\Delta_R < 0, \Delta_L = 0, \Sigma > 0$	≤ 1
$\Delta_R < 0, \Delta_L > 0, \Pi < 0$	≤ 1
$\Delta_R = 0, \Delta_L > 0, \Sigma < 0, \Pi < 0$	≤ 1
$\Delta_R > 0, \Delta_L > 0, \Sigma < 0, \Pi < 0$	≤ 1
Otherwise	$= 0$

TABLE VI: Constraints on the intersection number for the critical points ϕ_{\pm} when the action is \mathcal{PT} -symmetric.

The situation when $a \leq 0$ is far more delicate than the previous situations we have considered. In the region for the these values of the parameters, all the three critical points lie on the imaginary axis ($x = 0$). Further, one of the solutions to the thimble equation, Eq. (7), is $x = 0$. Since $c < 0$, this solution lies outside the regions of stability, and is an anti-thimble as illustrated in Fig. 7. The main assumption in deriving Eq. (3) was that the critical points do not share a common gradient flow. This assumption is violated when $a \leq 0$, and thus the intersection number cannot be determined using the method employed in our calculations.

¹⁰ We have only considered polynomials in ix but any function with real powers of ix is \mathcal{PT} -symmetric.

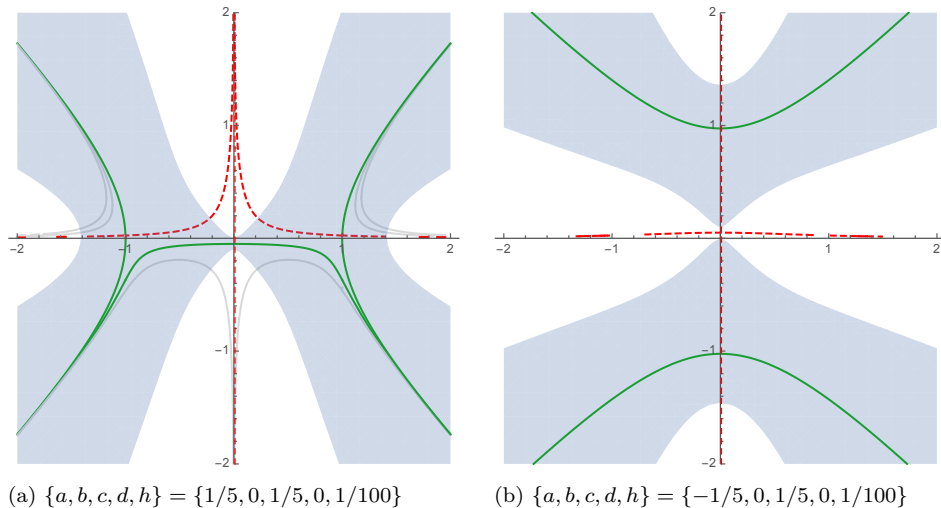


FIG. 7: (Colour online). Change in the structure of thimbles as the parameter a crosses the phase boundary $a = 0$. In both the figures, the green solid curves represent the thimbles, red dashed curves represent the anti-thimbles, and the grey solid curves represent the ghosts. The shaded regions represent the regions where $\text{Re}(S) \geq 0$. The anti-thimble $x = 0$ has been offset to $x = 0.01$ for better visibility. We see that there is a drastic change in the underlying thimble structure as the system passes through a phase transition.

VI. QUANTUM PHASE TRANSITION AND CHANGE IN THIMBLE STRUCTURE

In this section, we demonstrate the usefulness of the results in Sec. V with the help of a few examples. We choose to fix c , d , and h , and vary either a or b in order to maximize the number of conditions that need to be checked.

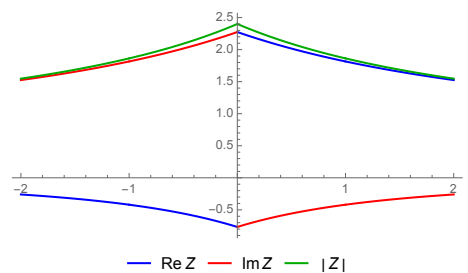
First, consider the situation where $\beta = 1$ and $h = 0$. Equation (34) tells us that the intersection number depends only on the relative sign of a and c , and that b has no effect on the intersection number. Thus, choosing $b = 1$ and plotting the partition function as a function of a , we clearly observe a discontinuity (or kink) at $a = 0$ as demonstrated in Fig. 8, and thus for the given choice of parameters, the system undergoes a phase transition at $a = 0$. Looking at the corresponding change to the structure of the thimbles, shown in Fig. 9, the discontinuity in Z is due to the change in the intersection number of ϕ_{\pm} from zero for $a > 0$ and one for each critical point when $a < 0$.

We now choose $a = 1$, $c = 1$, $d = 1$, and $h = 0$. The expressions in Eq. (35) in terms of b are

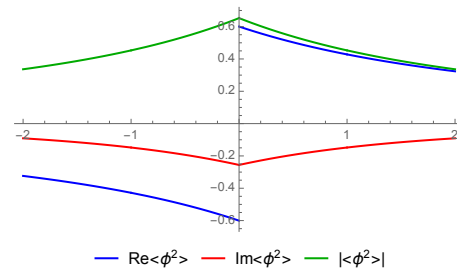
$$\Delta = \frac{(b-1)^2}{2}, \quad (51a)$$

$$\Pi = \frac{b^2 + 2b - 1}{2}, \quad (51b)$$

$$\Sigma = b. \quad (51c)$$



(a) The partition function



(b) The observable $\langle \phi^2 \rangle$

FIG. 8: (Colour online). The partition function Z and the observable $\langle \phi^2 \rangle$ as a function of a for the parameters $b = 1$, $c = 1$, $d = 0$, and $h = 0$. The blue curve represents the real part, the red curve represents the imaginary part, and the green curve represents the absolute value. Clearly, there is a discontinuity/kink at $a = 0$.

Based on the conditions given in Table I, we expect a sudden change in the value of the partition function when

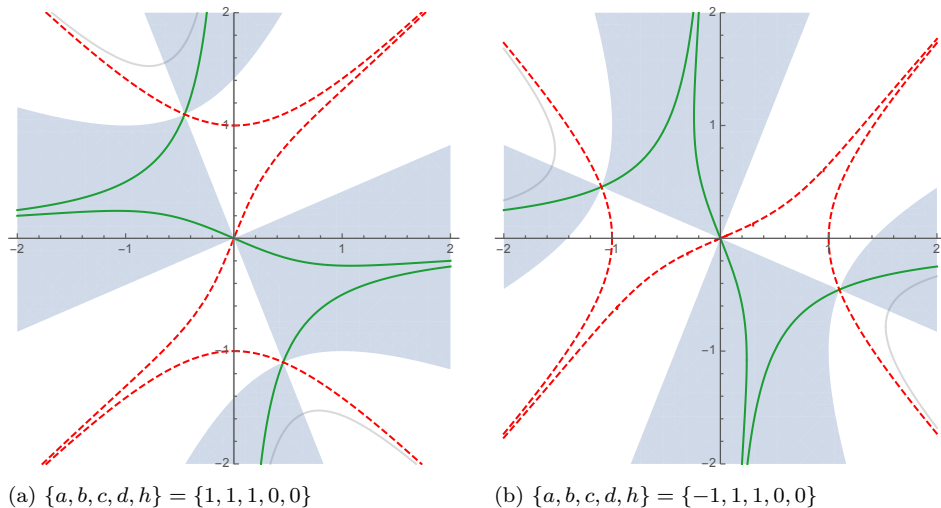


FIG. 9: (Colour online). Change in the structure of thimbles as the parameter a crosses the phase boundary $a = 0$. In both the figures, the green solid curves represent the thimbles, red dashed curves represent the anti-thimbles, and the grey solid curves represent the ghosts. The shaded regions represent the regions where $\text{Re}(S) \geq 0$. We see that there is a drastic change in the underlying thimble structure as the system passes through a phase transition.

$b = 0$. From Table II, we expect that this should happen when $b = 0, -1 - \sqrt{2}$. Note that although it seems like we can expect a phase transition around $b = 1$ and $b = -1 + \sqrt{2}$, in the vicinity of these points, the intersection number does not change. On plotting the partition function for these parameters, we observe a discontinuity at $b = -1 - \sqrt{2}$. (See Fig. 10.) The explanation for why we do not obtain a discontinuity is that at $b = 0$, the change in the number of solutions is reflected in $\langle \mathcal{J}_i, \mathbb{R} \rangle$ instead of $\langle \mathcal{K}_i, \mathbb{R} \rangle$. This explains why we have mentioned everywhere that the intersection number is less than or equal to a certain integer.

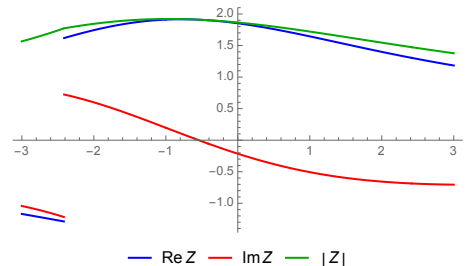
We can further complicate the situation and try to see where we observe discontinuities as we vary both a and b simultaneously. The expressions given in Eq. (35) in terms of a and b for $c = 1, d = 1$, and $h = 0$ are

$$\Delta = \frac{(b-a)^2}{8}, \quad (52a)$$

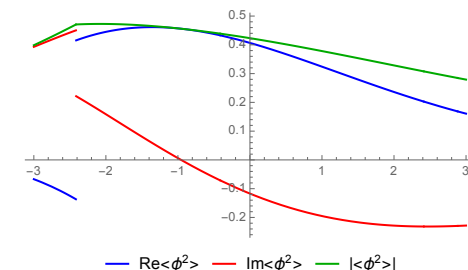
$$\Pi = \frac{b^2 + 2ab - a^2}{2}, \quad (52b)$$

$$\Sigma = b. \quad (52c)$$

A naive expectation would thus straightforwardly be that when $a = b$ or when $b^2 - a^2 + 2ab = 0$ (corresponding to the case $\Delta = 0$ and $\Pi = 0$), the partition function will have a discontinuity. (See Fig. 11.) Plotting the partition function as a function of a and b , we observe that this expectation is valid in certain cases, and in certain cases there is no discontinuity.



(a) The partition function



(b) The observable $\langle \phi^2 \rangle$

FIG. 10: (Colour online). The partition function Z and observable $\langle \phi^2 \rangle$ as a function of b for the parameters $a = 1, c = 1, d = 1$, and $h = 0$. The blue curve represents the real part, the red curve represents the imaginary part, and the green curve represents the absolute value. We observe a discontinuity at $b = -1 - \sqrt{2}$.

Let us now turn on the source term. We maintain $a = 1, c = 1$, and $d = 1$. Choosing $h = 0.01$, Eq. (10)

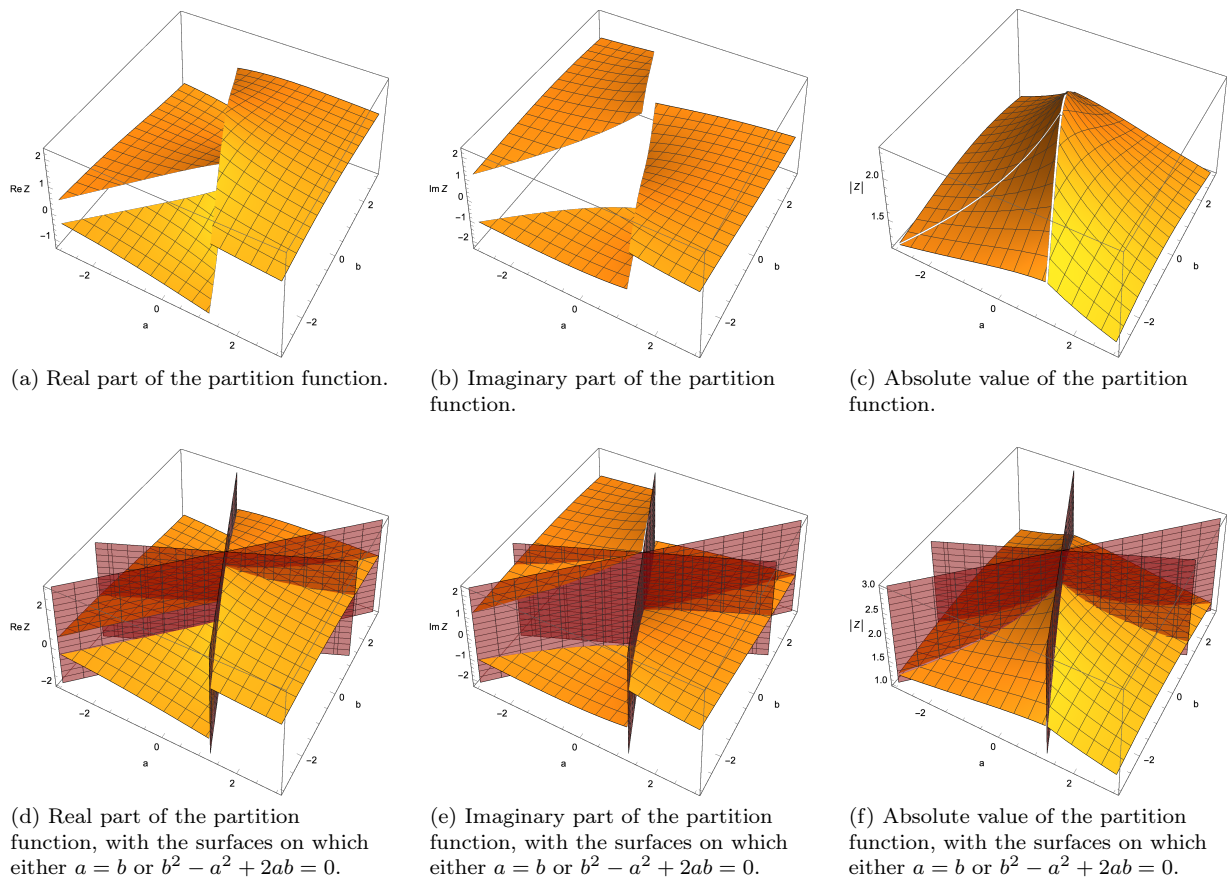


FIG. 11: (Colour online) Real, imaginary, and absolute values of the partition function as a function of a and b for the parameters $c = 1$, $d = 1$, and $h = 0$. The yellow surfaces represent the respective values of the partition function and the red surfaces represent the surface along which either $a = b$ or $b^2 - a^2 + 2ab = 0$.

becomes

$$\rho_0 = 0, \quad (53a)$$

$$\rho_+ = \frac{1 - b^2 - 2b}{8} + 0.01\Omega, \quad (53b)$$

$$\rho_- = \frac{1 - b^2 - 2b}{8} - 0.01\Omega, \quad (53c)$$

where

$$\Omega = \sqrt{b^2 + 1} \cos \left[\arctan \left(\frac{b-1}{b+1} \right) \right]. \quad (54)$$

We do not expect a phase transition with respect to ϕ_0 since here $\rho_0 = 0$, and we have already fixed our choice of a and c . Corresponding to the critical points ϕ_+ and

ϕ_- , we have, from Eq. (36)

$$\Delta_+ = \frac{b^2 - 2b + 1}{2} + 0.04\Omega, \quad (55a)$$

$$\Delta_- = \frac{b^2 - 2b + 1}{2} - 0.04\Omega, \quad (55b)$$

$$\Pi_+ = \frac{1 - b^2 - 2b}{8} + 0.01\Omega, \quad (55c)$$

$$\Pi_- = \frac{1 - b^2 - 2b}{8} - 0.01\Omega, \quad (55d)$$

$$\Sigma = b. \quad (55e)$$

As is evident, when the source term is real, the equivalence between the critical points ϕ_+ and ϕ_- gets lifted while ϕ_0 remains untouched. Solving the equations using a symbol interpreter, we get the points where the phase transitions could be expected as

$$b = \begin{cases} 0 & (\text{if } \Sigma = 0), \\ 1 + \frac{1}{(25\sqrt{2})} \pm 12\sqrt{\frac{2}{625} + \frac{8\sqrt{2}}{25}} & (\text{if } \Delta_- = 0), \\ -1 \pm \frac{1}{25}\sqrt{1251 - \sqrt{2501}} & (\text{if } \Pi_+ = 0), \\ -1 \pm \frac{1}{25}\sqrt{1251 + \sqrt{2501}} & (\text{if } \Pi_- = 0), \end{cases} \quad (56)$$

Numericising the above values of b , we get

$$b = \{0, 0.6907, 1.3658, -2.3862, \\ 0.3862, -2.4428, 0.4428\}. \quad (57)$$

The partition function for this action, from Eq. (25), is given as

$$Z = I_0 + \frac{h^2}{2}I_2 + \mathcal{O}(h^4) \quad (58)$$

$$= I_0 + 0.00005I_2. \quad (59)$$

This has a discontinuity in the vicinity of $b = -2.4$. However, the point at which the partition function is discontinuous does not match exactly with either $b = -2.38621$ or $b = -2.44278$. In fact, it matches exactly with our previous example where the boundary was at $b = -1 - \sqrt{2}$. We believe the issue is with the expansion of Z_{sources} and not the method used to find the points of phase transitions, due to the fact that the perturbative expansion with respect to h in Eq. (25) depends on the partition function and observables of the action without sources. These are not sensitive to the lifting of equivalence between ϕ_+ and ϕ_- .

VII. SUMMARY OF RESULTS

We have presented a lot of small results in the previous sections. Let us summarize them and put them into perspective.

For an action in zero dimensions with scalar fields, where the information about the background manifold is irrelevant¹¹ and the complexified degrees of freedom of the fields are in \mathbb{C} , the thimbles can be found analytically by exploiting the most crucial property of these curves – the imaginary part of the action remains constant on them. However, solving for the thimbles using this method has its own problems as illustrated in Sec. IV where for more general situations, it is difficult to clearly distinguish between the solutions as they can either be thimbles or anti-thimbles, based on the region in the complex plane under question. We called this the ‘piecewise behavior’ of the solutions. The method is also extremely restricted to a small set of toy problems since it is only valid for polynomial actions of order less than five in zero dimensions. It would be interesting to comment about the piecewise behavior of thimbles when dealing with models in higher dimensions.

Despite these issues, there are advantages of employing the Lefschetz thimbles method since it provides a lot of ancillary information about the system. Since the weights in Eq. (2) are in general integers, changes in the weights correspond to discontinuities in the partition function, indicating the existence of different phases. We

used the simple method of solving Eq. (7), massaged in a way to access the information on the weights as outlined in Sec. V and Appendix A, to find conditional expressions involving relations between the parameters of the system that characterize the different phases of the system. A few examples showcasing the effectiveness of this method was presented in Sec. VI.

Although from the results, it is evident that phase transitions occur in the system, comments on the thermodynamical nature of these transitions cannot be made for the model we have chosen since thermodynamic quantities such as the free energy cannot be consistently defined in zero dimensions. However, there are two main observations about the behaviour of the phases. First, the boundaries of phase transitions are completely determined by the parameters h , α , and β . Thus, any symmetry involving the field ϕ remains a symmetry post phase transition. Second, these phase transition boundaries correspond to distinct changes in the topological structure of the thimbles and anti-thimbles. (We show this feature in Fig. 9.) These observations are a clear indication of the existence of “quantum phases” and “quantum phase transitions” [20, 39, 54, 63, 64]. Further, regions within the phase boundaries are akin to wall chambers and a phase transition corresponds to wall crossing.

We also, in passing, mentioned how looking at the action with sources as a perturbative expansion in terms of the action without sources fails, which was not obvious in Eq. (25) but emerged during our demonstration in Sec. VI. This further validates the power of using Lefschetz thimbles when compared to simple, perturbative analysis of systems.

VIII. CONCLUSIONS AND FUTURE DIRECTIONS

Although the Lefschetz thimbles formalism is a great mathematical tool to deal with the sign problem in quantum field theories with complex actions, performing actual calculations might involve many difficulties. The flow equation, Eq. (1), even in its zero-dimensional version, Eq. (4), is in general very difficult to solve since it involves complex variables. In this paper, we instead exploited the properties of these thimbles to analytically demonstrate how the Lefschetz thimbles formalism can be used to predict phase transitions for scalar theories in zero dimensions, and connected it to quantum phase transitions. An immediate extension would be to explore the same problem for supersymmetric theories in zero dimensions. The logarithmic term in the effective action, once the fermionic degrees of freedom have been integrated out, could lead to a few issues due to a pesky arctan term in Eq. (10). We still believe that the system would be solvable, post a few clever deformations that mitigate the problem of dealing with the arctan.

The definition of the thimble and anti-thimble also makes it difficult to solve numerically since any large

¹¹ Rather, non-existent.

number as the choice for the parameter t in Eq. (1), that is not infinity, will give a constant solution. An alternative has been suggested to deal with the issue by introducing a computational parameter that makes the flow equation easier to handle computationally [65]. Further, there are computational tools in place to heuristically find these thimbles using Monte Carlo methods [66–69], which seem to have some success in finding these thimbles without having to solve the flow equation. However, these solutions are numerical in nature, and in general it is very difficult to find these thimbles analytically.

In zero dimensions, except for showing that the partition function and observables develop discontinuities, comments on the thermodynamical nature of phase transitions cannot be made. Thus a more non-trivial and highly elucidatory extension would be to study phase transitions in higher dimensional systems, where the information of the background manifold becomes important and thermodynamic quantities can be defined consistently. There has been some success in effecting these calculations numerically using hybrid Monte Carlo simulations for the one-dimensional Thirring model [70], and there are numerous demonstrations of connections between Lee-Yang zeroes and Stokes phenomena in the context of chiral phase transitions [63, 64, 71, 72]. However, a completely analytic and general demonstration of phase structures of higher dimensional systems, their relation to the structure of thimbles/anti-thimbles, and a relation with the thermodynamics of the system if any, is desired.

ACKNOWLEDGMENTS

The work of AJ was supported in part by the Startup Research Grant (No. SRG/2019/002035) from the Science & Engineering Research Board (SERB), Government of India, and in part by a Seed Grant from the Indian Institute of Science Education and Research (IISER) Mohali. The work of RB was partially supported by an INSPIRE Scholarship for Higher Education by the Department of Science and Technology, Government of India. A part of this work was presented by RB at the Science Undergraduate Research Conference at Azim Premji University, Bangalore, India in December 2019.

Appendix A: Expressions for Boundaries of Phase Transitions

In this section we derive the expressions for the boundaries of phase transitions. We start with the case where the source parameter h is zero. The imaginary part of the action is

$$\begin{aligned} \text{Im } S(x, y) &= \frac{d}{4}y^4 - cxy^3 - \left(\frac{b}{2} + \frac{3d}{2}x^2\right)y^2 \\ &+ (ax + cx^3)y + \frac{b}{2}x^2 + \frac{d}{4}x^4, \end{aligned} \quad (\text{A1})$$

and the critical points of the action are

$$\phi_0 = 0, \quad (\text{A2})$$

$$\phi_{\pm} = \pm i\sqrt{\frac{\alpha}{\beta}}. \quad (\text{A3})$$

Along the original integration cycle, \mathbb{R} , which corresponds to $y = 0$, the imaginary part of the action is

$$\text{Im } S(x) = \frac{b}{2}x^2 + \frac{d}{4}x^4. \quad (\text{A4})$$

To get the combined intersection number of the thimble and anti-thimble of a critical point, we look for the existence of real solutions to the equation

$$\frac{b}{2}x^2 + \frac{d}{4}x^4 - \rho_i = 0. \quad (\text{A5})$$

Here, $\rho_i = \text{Im } S$ at ϕ_i , see Eq. (10). In the case where $d = 0$, Eq. (A5) is simply

$$x = \pm\sqrt{\frac{2\rho_i}{b}}. \quad (\text{A6})$$

Substituting ρ_i , the above equation takes the form

$$x = \begin{cases} 0 & \text{when } i = 0, \\ \pm\sqrt{-\frac{a}{c}} & \text{when } i = \pm. \end{cases} \quad (\text{A7})$$

Requiring $x \in \mathbb{R}$ and using $\langle \mathcal{J}_i, \mathcal{K}_{i'} \rangle = \delta_{i,i'}$, this immediately gives us

$$n_i \begin{cases} = 1 & \text{when } i = 0, \forall \alpha, \beta, \\ \leq 1 & \text{when } i = \pm, \frac{a}{c} < 0, \\ = 0 & \text{when } i = \pm, \frac{a}{c} > 0. \end{cases} \quad (\text{A8})$$

When $d \neq 0$, Eq. (A5) is a bi-quadratic. Defining $w = x^2$, we look for *positive* real solutions to

$$\frac{b}{2}w + \frac{d}{4}w^2 - \rho_i = 0. \quad (\text{A9})$$

The relevant parameters associated with the above equation are its discriminant, sum of roots, and product of roots. Denoting them as Δ , $-\Sigma$, and Π respectively¹², we obtain

$$\Delta = \frac{(bc - ad)^2}{(c^2 + d^2)}, \quad (\text{A10})$$

$$\Pi = \frac{d(b^2 - a^2) + 2abc}{d(c^2 + d^2)}, \quad (\text{A11})$$

$$\Sigma = \frac{b}{d}. \quad (\text{A12})$$

It is to be noted that we have chosen to omit overall factors (such as that of 2 in Σ) since what is relevant

¹² We use $-\Sigma$ for sum of roots to avoid dealing with an overall minus sign in our results.

is only the sign of these quantities. When the discriminant is positive, we have two distinct real solutions for w . In this case, when the product of roots is positive, either both solutions are positive (giving a combined intersection number of 4) or both solutions are negative (intersection number is zero). This is checked using Σ . When the discriminant is zero, we only get one real root for w . Again, Σ helps in determining whether the root is positive or negative. When the discriminant is negative (which for this particular case is never possible), there are no real roots of w and the intersection number is zero. These end up giving the conditions mentioned in Tables I and II.

When the source term is non-zero, and the parameter h is real, the analysis remains exactly the same. The only change is the change to ρ_i . If the source term is purely imaginary, Eq. (A4) now becomes

$$hx + \frac{b}{2}x^2 + \frac{d}{4}x^4 + \rho_i = 0. \quad (\text{A13})$$

Since the equation is now a purely quartic equation (in the sense that it is not reducible to a bi-quadratic), we have a complicated set of conditions for n_i . We refer the reader to the conditions in Ref. [58] to arrive at the results in Table IV.

When the action possesses \mathcal{PT} -symmetry, we can obtain its critical points and the imaginary part of the action by substituting $h \rightarrow ih$ and $c \rightarrow -c$ in Eqs. (8) and (10), which gives us

$$\phi_0 = -\frac{ih}{a} + \mathcal{O}(h^3), \quad (\text{A14})$$

$$\phi_{\pm} = \pm \sqrt{\frac{a}{c}} - \frac{ih}{2a} \pm \frac{3h^2}{8} \sqrt{\frac{c}{a^5}} + \mathcal{O}(h^3). \quad (\text{A15})$$

$$\rho_i = \begin{cases} 0 & \text{when } a \leq 0, \forall i, \\ 0 & \text{when } a > 0, i = 0, \\ -h\sqrt{\frac{a}{|c|}} & \text{when } a > 0, i = +, \\ +h\sqrt{\frac{a}{|c|}} & \text{when } a > 0, i = -. \end{cases} \quad (\text{A16})$$

The imaginary part of the action, given in Eq. (A1), upon making these substitutions becomes

$$\text{Im } S(x, y) = hx + axy - c(x^3y - xy^3). \quad (\text{A17})$$

As outlined in Sec. III, the standard procedure for dealing with this action is to take an integration cycle about the angles $5\pi/4$ and $7\pi/4$ (in the third and the fourth quadrant, respectively). We have chosen it to be (See Eq. (11))

$$y(x) = \begin{cases} x & \text{for } x \leq 0, \\ -x & \text{for } x > 0. \end{cases} \quad (\text{A18})$$

Substituting the above integration cycle in Eq. (A17) and equating it to the imaginary part of the action at a critical point, we obtain

$$hx + ax^2 + \rho_i = 0 \quad \text{for } x \leq 0, \quad (\text{A19})$$

$$hx - ax^2 + \rho_i = 0 \quad \text{for } x > 0. \quad (\text{A20})$$

Condition	Intersection number
$\Delta_L > 0, \Pi_L > 0, \Sigma_L < 0$	≤ 2
$\Delta_L = 0, \Sigma_L < 0$	≤ 1
$\Delta_L > 0, \Pi_L < 0$	≤ 1
Otherwise	$= 0$

TABLE VII: The ‘Left’ intersection number n_i^L for critical points ϕ_0 and ϕ_{\pm} when the action is \mathcal{PT} -symmetric.

For the case where $a > 0$, we split the intersection number into two parts. The number of times the thimble and anti-thimble intersect the part of the integration cycle where $x < 0$ is called n_i^L , and the number of times the thimble and anti-thimble intersect the part of the integration cycle where $x > 0$ is called n_i^R . The total intersection number thus is $n_i = n_i^L + n_i^R$. For $x < 0$, since the associated (anti-)thimble equation is a quadratic in x , we define the discriminant, product of roots, and sum of roots as

$$\Delta_L = h^2 - 4a\rho_i, \quad (\text{A21})$$

$$\Pi_L = \frac{\rho_i}{a}, \quad (\text{A22})$$

$$\Sigma_L = -\frac{h}{2a}. \quad (\text{A23})$$

We obtain similar expressions for $x > 0$

$$\Delta_R = h^2 + 4a\rho_i, \quad (\text{A24})$$

$$\Pi_R = -\frac{\rho_i}{a}, \quad (\text{A25})$$

$$\Sigma_R = \frac{h}{2a}. \quad (\text{A26})$$

Here we look for negative real solutions for the Eq. (A19) and positive real solutions for the Eq. (A20). Standard analysis of quadratic equations gives us the conditional expressions in Tables VIII and VIII.

Condition	Intersection number
$\Delta_R > 0, \Pi_R > 0, \Sigma_R > 0$	≤ 2
$\Delta_R = 0, \Sigma_R > 0$	≤ 1
$\Delta_R > 0, \Pi_R < 0$	≤ 1
Otherwise	$= 0$

TABLE VIII: The ‘Right’ intersection number n_i^R for critical points ϕ_0 and ϕ_{\pm} when the action is \mathcal{PT} -symmetric.

Combining these conditions is slightly non-trivial since there are cases where two conditional expressions cannot

be satisfied simultaneously. (For example, $\Sigma_L > 0$ and $\Sigma_R > 0$ is not simultaneously possible.) Having taken

care of such situations, we arrive at the results in Table VI.

-
- [1] C. M. Bender and S. Boettcher, “Real spectra in nonHermitian Hamiltonians having PT symmetry,” *Phys. Rev. Lett.* **80** (1998) 5243–5246, [arXiv:physics/9712001 \[physics\]](#).
- [2] C. M. Bender, D. C. Brody, and H. F. Jones, “Complex extension of quantum mechanics,” *Phys. Rev. Lett.* **89** (2002) 270401, [arXiv:quant-ph/0208076 \[quant-ph\]](#). [Erratum: *Phys. Rev. Lett.* **92**, 119902 (2004)].
- [3] C. M. Bender, “Introduction to PT-Symmetric Quantum Theory,” *Contemp. Phys.* **46** (2005) 277–292, [arXiv:quant-ph/0501052 \[QUANT-PH\]](#).
- [4] E. Witten, “Analytic Continuation Of Chern-Simons Theory,” *arXiv:1001.2933 [hep-th]* (Aug., 2010). <http://arxiv.org/abs/1001.2933>. [arXiv: 1001.2933](#).
- [5] E. Witten, “A New Look At The Path Integral Of Quantum Mechanics,” *arXiv:1009.6032 [hep-th]* (Sept., 2010). <http://arxiv.org/abs/1009.6032>. [arXiv: 1009.6032](#).
- [6] G. Aarts, F. A. James, E. Seiler, and I.-O. Stamatescu, “Complex Langevin: Etiology and Diagnostics of its Main Problem,” *Eur. Phys. J. C* **71** (2011) 1756, [arXiv:1101.3270 \[hep-lat\]](#).
- [7] G. Aarts, F. A. James, J. M. Pawłowski, E. Seiler, D. Sexty, and I.-O. Stamatescu, “Stability of complex Langevin dynamics in effective models,” *JHEP* **03** (2013) 073, [arXiv:1212.5231 \[hep-lat\]](#).
- [8] G. Aarts, “Complex Langevin dynamics and other approaches at finite chemical potential,” *PoS LATTICE2012* (2012) 017, [arXiv:1302.3028 \[hep-lat\]](#).
- [9] G. Aarts, L. Bongiovanni, E. Seiler, D. Sexty, and I.-O. Stamatescu, “Controlling complex Langevin dynamics at finite density,” *Eur. Phys. J. A* **49** (2013) 89, [arXiv:1303.6425 \[hep-lat\]](#).
- [10] J. Nishimura and S. Shimasaki, “New Insights into the Problem with a Singular Drift Term in the Complex Langevin Method,” *Phys. Rev. D* **92** no. 1, (2015) 011501, [arXiv:1504.08359 \[hep-lat\]](#).
- [11] Y. Ito and J. Nishimura, “The complex Langevin analysis of spontaneous symmetry breaking induced by complex fermion determinant,” *JHEP* **12** (2016) 009, [arXiv:1609.04501 \[hep-lat\]](#).
- [12] J. Nishimura and S. Shimasaki, “Combining the complex Langevin method and the generalized Lefschetz-thimble method,” *JHEP* **06** (2017) 023, [arXiv:1703.09409 \[hep-lat\]](#).
- [13] P. Basu, K. Jaswin, and A. Joseph, “Complex Langevin Dynamics in Large N Unitary Matrix Models,” *Phys. Rev. D* **98** no. 3, (2018) 034501, [arXiv:1802.10381 \[hep-th\]](#).
- [14] A. Joseph and A. Kumar, “Complex Langevin Simulations of Zero-dimensional Supersymmetric Quantum Field Theories,” *Phys. Rev. D* **100** (2019) 074507, [arXiv:1908.04153 \[hep-th\]](#).
- [15] G. Guralnik and Z. Guralnik, “Complexified path integrals and the phases of quantum field theory,” *Annals Phys.* **325** (2010) 2486–2498, [arXiv:0710.1256 \[hep-th\]](#).
- [16] G. Alexanian, R. MacKenzie, M. B. Paranjape, and J. Ruel, “Path integration and perturbation theory with complex Euclidean actions,” *Phys. Rev. D* **77** (2008) 105014, [arXiv:0802.0354 \[hep-th\]](#).
- [17] A. Denbleyker, D. Du, Y. Liu, Y. Meurice, and H. Zou, “Fisher’s zeros as boundary of renormalization group flows in complex coupling spaces,” *Phys. Rev. Lett.* **104** (2010) 251601, [arXiv:1005.1993 \[hep-lat\]](#).
- [18] K. Nagao and H. B. Nielsen, “Formulation of Complex Action Theory,” *Prog. Theor. Phys.* **126** (2011) 1021–1049, [arXiv:1104.3381 \[quant-ph\]](#). [Erratum: *Prog. Theor. Phys.* **127**, 1131 (2012)].
- [19] D. Harlow, J. Maltz, and E. Witten, “Analytic Continuation of Liouville Theory,” *JHEP* **12** (2011) 071, [arXiv:1108.4417 \[hep-th\]](#).
- [20] D. D. Ferrante, G. S. Guralnik, Z. Guralnik, and C. Pehlevan, “Complex Path Integrals and the Space of Theories,” in *Miami 2010: Topical Conference on Elementary Particles, Astrophysics, and Cosmology Fort Lauderdale, Florida, USA, December 14-19, 2010*. 2013. [arXiv:1301.4233 \[hep-th\]](#).
- [21] H. Nishimura, M. C. Ogilvie, and K. Pangeni, “Complex saddle points in QCD at finite temperature and density,” *Phys. Rev. D* **90** no. 4, (2014) 045039, [arXiv:1401.7982 \[hep-ph\]](#).
- [22] Y. Tanizaki and T. Koike, “Real-time Feynman path integral with Picard-Lefschetz theory and its applications to quantum tunneling,” *Annals Phys.* **351** (2014) 250–274, [arXiv:1406.2386 \[math-ph\]](#).
- [23] A. Cherman and M. Unsal, “Real-Time Feynman Path Integral Realization of Instantons,” [arXiv:1408.0012 \[hep-th\]](#).
- [24] D. Sexty, “New algorithms for finite density QCD,” *PoS LATTICE2014* (2014) 016, [arXiv:1410.8813 \[hep-lat\]](#).
- [25] Y. Tanizaki, “Lefschetz-thimble techniques for path integral of zero-dimensional $O(n)$ sigma models,” *Phys. Rev. D* **91** no. 3, (2015) 036002, [arXiv:1412.1891 \[hep-th\]](#).
- [26] AuroraScience Collaboration, M. Cristoforetti, F. Di Renzo, and L. Scorzato, “New approach to the sign problem in quantum field theories: High density QCD on a Lefschetz thimble,” *Phys. Rev. D* **86** (2012) 074506, [arXiv:1205.3996 \[hep-lat\]](#).
- [27] M. Cristoforetti, F. Di Renzo, G. Erucci, A. Mukherjee, C. Schmidt, L. Scorzato, and C. Torrero, “An efficient method to compute the residual phase on a Lefschetz thimble,” *Phys. Rev. D* **89** no. 11, (2014) 114505, [arXiv:1403.5637 \[hep-lat\]](#).
- [28] M. Cristoforetti, F. Di Renzo, A. Mukherjee, and L. Scorzato, “Monte Carlo simulations on the Lefschetz thimble: Taming the sign problem,” *Phys. Rev. D* **88** no. 5, (2013) 051501, [arXiv:1303.7204 \[hep-lat\]](#).
- [29] A. Mukherjee, M. Cristoforetti, and L. Scorzato, “Metropolis Monte Carlo integration on the Lefschetz thimble: Application to a one-plaquette model,” *Phys.*

- Rev.* **D88** no. 5, (2013) 051502, [arXiv:1308.0233](https://arxiv.org/abs/1308.0233) [physics.comp-ph].
- [30] G. Aarts, “Lefschetz thimbles and stochastic quantization: Complex actions in the complex plane,” *Phys. Rev.* **D88** no. 9, (2013) 094501, [arXiv:1308.4811](https://arxiv.org/abs/1308.4811) [hep-lat].
- [31] H. Fujii, D. Honda, M. Kato, Y. Kikukawa, S. Komatsu, and T. Sano, “Hybrid Monte Carlo on Lefschetz thimbles - A study of the residual sign problem,” *JHEP* **10** (2013) 147, [arXiv:1309.4371](https://arxiv.org/abs/1309.4371) [hep-lat].
- [32] T. Kanazawa and Y. Tanizaki, “Structure of Lefschetz thimbles in simple fermionic systems,” *JHEP* **03** (2015) 044, [arXiv:1412.2802](https://arxiv.org/abs/1412.2802) [hep-th].
- [33] H. Fujii, S. Kamata, and Y. Kikukawa, “Lefschetz thimble structure in one-dimensional lattice Thirring model at finite density,” *JHEP* **11** (2015) 078, [arXiv:1509.08176](https://arxiv.org/abs/1509.08176) [hep-lat]. [Erratum: *JHEP* **02**, 036 (2016)].
- [34] A. Alexandru, G. Basar, and P. Bedaque, “Monte Carlo algorithm for simulating fermions on Lefschetz thimbles,” *Phys. Rev.* **D93** no. 1, (2016) 014504, [arXiv:1510.03258](https://arxiv.org/abs/1510.03258) [hep-lat].
- [35] F. Di Renzo and G. Eruzzi, “One-dimensional QCD in thimble regularization,” *Phys. Rev.* **D97** no. 1, (2018) 014503, [arXiv:1709.10468](https://arxiv.org/abs/1709.10468) [hep-lat].
- [36] T. Fujimori, M. Honda, S. Kamata, T. Misumi, and N. Sakai, “Resurgence and Lefschetz thimble in three-dimensional $\mathcal{N} = 2$ supersymmetric Chern-Simons matter theories,” *PTEP* **2018** no. 12, (2018) 123B03, [arXiv:1805.12137](https://arxiv.org/abs/1805.12137) [hep-th].
- [37] Y. Tanizaki, Y. Hidaka, and T. Hayata, “Lefschetz-thimble approach to the Silver Blaze problem of one-site fermion model,” *PoS LATTICE2016* (2016) 030, [arXiv:1610.00393](https://arxiv.org/abs/1610.00393) [hep-lat].
- [38] G. V. Dunne and M. Ünsal, “Resurgence and Trans-series in Quantum Field Theory: The CP(N-1) Model,” *JHEP* **11** (2012) 170, [arXiv:1210.2423](https://arxiv.org/abs/1210.2423) [hep-th].
- [39] G. Basar, G. V. Dunne, and M. Ünsal, “Resurgence theory, ghost-instantons, and analytic continuation of path integrals,” *JHEP* **10** (2013) 041, [arXiv:1308.1108](https://arxiv.org/abs/1308.1108) [hep-th].
- [40] A. Cherman, D. Dorigoni, and M. Ünsal, “Decoding perturbation theory using resurgence: Stokes phenomena, new saddle points and Lefschetz thimbles,” *JHEP* **10** (2015) 056, [arXiv:1403.1277](https://arxiv.org/abs/1403.1277) [hep-th].
- [41] A. Cherman, P. Koroteev, and M. Ünsal, “Resurgence and Holomorphy: From Weak to Strong Coupling,” *J. Math. Phys.* **56** no. 5, (2015) 053505, [arXiv:1410.0388](https://arxiv.org/abs/1410.0388) [hep-th].
- [42] D. Dorigoni, “An Introduction to Resurgence, Trans-Series and Alien Calculus,” *Annals Phys.* **409** (2019) 167914, [arXiv:1411.3585](https://arxiv.org/abs/1411.3585) [hep-th].
- [43] A. Banyaga and D. Hurtubise, *Lectures on Morse Homology*. Texts in the Mathematical Sciences. Springer Netherlands, 2013. <https://books.google.co.in/books?id=W8PcBwAAQBAJ>.
- [44] F. Pham, “Vanishing homologies and the n variables saddlepoint method,” in *Proc. Symp. Pure Math.*, vol. 40, pp. 310–333. 1983.
- [45] V. I. Arnold, A. N. Varchenko, and S. M. Gusein-Zade, *Singularities of Differentiable Maps: Volume II Monodromy and Asymptotic Integrals*, vol. 83. Springer Science & Business Media, 2012.
- [46] Y. Tanizaki, *Study on sign problem via Lefschetz-thimble path integral*. PhD thesis, Tokyo U., Dec., 2015. <http://hdl.handle.net/2261/00073296>.
- [47] M. Cristoforetti, F. Di Renzo, and L. Scorzato, “High density QCD on a Lefschetz thimble?,” *Phys. Rev. D* **86** no. 7, (Oct., 2012) 074506. [http://arxiv.org/abs/1205.3996](https://arxiv.org/abs/1205.3996). [arXiv: 1205.3996](https://arxiv.org/abs/1205.3996).
- [48] A. Duncan and M. Niedermaier, “Temporal breakdown and Borel resummation in the complex Langevin method,” *Annals of Physics* **329** (Feb., 2013) 93–124. [http://arxiv.org/abs/1205.0307](https://arxiv.org/abs/1205.0307). [arXiv: 1205.0307](https://arxiv.org/abs/1205.0307).
- [49] G. Aarts, P. Giudice, and E. Seiler, “Localised distributions and criteria for correctness in complex Langevin dynamics,” *Annals of Physics* **337** (Oct., 2013) 238–260. [http://arxiv.org/abs/1306.3075](https://arxiv.org/abs/1306.3075). [arXiv: 1306.3075](https://arxiv.org/abs/1306.3075).
- [50] N. H. Abel, “Mémoire sur les équations algébriques, ou l’on démontre l’impossibilité de la résolution de l’équation générale du cinquième degré,” *Œuvres Complètes de Niels Henrik Abel (in French)* **I** 28–33.
- [51] N. H. Abel, “Démonstration de l’impossibilité de la résolution algébrique des équations générales qui passent le quatrième degré,” *Œuvres Complètes de Niels Henrik Abel (in French)* **I** 66–87.
- [52] P. Ruffini, “Teoria generale delle equazioni, in cui si dimostra impossibile la soluzione algebraica delle equazioni generali di grado superiore al quarto,” *Stamperia di S. Tommaso d’Aquino (in Italian)* (1799) .
- [53] G. V. Dunne and M. Ünsal, “What is QFT? Resurgent trans-series, Lefschetz thimbles, and new exact saddles,” *PoS LATTICE2015* (2016) 010, [arXiv:1511.05977](https://arxiv.org/abs/1511.05977) [hep-lat].
- [54] A. Cherman, D. Dorigoni, and M. Ünsal, “Decoding perturbation theory using resurgence: Stokes phenomena, new saddle points and lefschetz thimbles,” [arXiv:1403.1277](https://arxiv.org/abs/1403.1277) [hep-th].
- [55] C. M. Bender, “Making Sense of Non-Hermitian Hamiltonians,” *Rep. Prog. Phys.* **70** no. 6, (June, 2007) 947–1018. [http://arxiv.org/abs/hep-th/0703096](https://arxiv.org/abs/hep-th/0703096). [arXiv: hep-th/0703096](https://arxiv.org/abs/hep-th/0703096).
- [56] C. M. Bender, D. C. Brody, J.-H. Chen, H. F. Jones, K. A. Milton, and M. C. Ogilvie, “Equivalence of a Complex \mathcal{PT} -Symmetric Quartic Hamiltonian and a Hermitian Quartic Hamiltonian with an Anomaly,” *Phys. Rev. D* **74** no. 2, (July, 2006) 025016. [http://arxiv.org/abs/hep-th/0605066](https://arxiv.org/abs/hep-th/0605066). [arXiv: hep-th/0605066](https://arxiv.org/abs/hep-th/0605066).
- [57] G. Aarts, “Lefschetz thimbles and stochastic quantisation: Complex actions in the complex plane,” *Phys. Rev. D* **88** no. 9, (Nov., 2013) 094501. [http://arxiv.org/abs/1308.4811](https://arxiv.org/abs/1308.4811). [arXiv: 1308.4811](https://arxiv.org/abs/1308.4811).
- [58] E. L. Rees, “Graphical Discussion of the Roots of a Quartic Equation,” *The American Mathematical Monthly* **29** no. 2, (Feb., 1922) 51–55. <https://www.tandfonline.com/doi/full/10.1080/00029890.1922.11986100>.
- [59] Y. Abe and K. Fukushima, “Analytical studies of the complex Langevin equation with a Gaussian Ansatz and multiple solutions in the unstable region,” *Phys. Rev. D* **94** no. 9, (Nov., 2016) 094506. [http://arxiv.org/abs/1607.05436](https://arxiv.org/abs/1607.05436). [arXiv: 1607.05436](https://arxiv.org/abs/1607.05436).
- [60] I. Aniceto, G. Başar, and R. Schiappa, “A Primer on Resurgent Transseries and Their Asymptotics,” [arXiv:1802.10441](https://arxiv.org/abs/1802.10441) [hep-lat, physics.hep-ph],

- physics:hep-th, physics:math-ph, physics:quant-ph*
(Jan., 2019) . <http://arxiv.org/abs/1802.10441>.
arXiv: 1802.10441.
- [61] K. F. Riley, M. P. Hobson, and S. J. Bence,
*Mathematical Methods for Physics and Engineering: A
Comprehensive Guide*. Cambridge University Press,
2 ed., 2002.
- [62] K. Fukushima and Y. Tanizaki, “Hamilton dynamics for
the Lefschetz thimble integration akin to the complex
Langevin method,” *Progress of Theoretical and
Experimental Physics* **2015** no. 11, (Nov., 2015)
111A01–111A01. <http://arxiv.org/abs/1507.07351>.
arXiv: 1507.07351.
- [63] G. Guralnik and Z. Guralnik, “Complexified Path
Integrals and the Phases of Quantum Field Theory,”
Annals of Physics **325** no. 11, (Nov., 2010) 2486–2498.
<http://arxiv.org/abs/0710.1256>. arXiv: 0710.1256.
- [64] T. Kanazawa and Y. Tanizaki, “Structure of Lefschetz
thimbles in simple fermionic systems,” *J. High Energ.
Phys.* **2015** no. 3, (Mar., 2015) 44.
<http://arxiv.org/abs/1412.2802>. arXiv: 1412.2802.
- [65] Y. Tanizaki, H. Nishimura, and J. J. M. Verbaarschot,
“Gradient flows without blow-up for Lefschetz
thimbles,” *J. High Energ. Phys.* **2017** no. 10, (Oct.,
2017) 100. <http://arxiv.org/abs/1706.03822>. arXiv:
1706.03822.
- [66] M. Cristoforetti, F. Di Renzo, A. Mukherjee, and
L. Scorzato, “Monte carlo simulations on the lefschetz
thimble: Taming the sign problem,” *Phys. Rev. D* **88**
(Sep, 2013) 051501. [https:
//link.aps.org/doi/10.1103/PhysRevD.88.051501](https://link.aps.org/doi/10.1103/PhysRevD.88.051501).
- [67] H. Fujii, D. Honda, M. Kato, Y. Kikukawa, S. Komatsu,
and T. Sano, “Hybrid monte carlo on lefschetz thimbles
? a study of the residual sign problem,” *Journal of High
Energy Physics* **2013** no. 10, (Oct, 2013) .
[http://dx.doi.org/10.1007/JHEP10\(2013\)147](http://dx.doi.org/10.1007/JHEP10(2013)147).
- [68] A. Alexandru, G. Basar, and P. Bedaque, “Monte carlo
algorithm for simulating fermions on lefschetz
thimbles,” *Phys. Rev. D* **93** (Jan, 2016) 014504. [https:
//link.aps.org/doi/10.1103/PhysRevD.93.014504](https://link.aps.org/doi/10.1103/PhysRevD.93.014504).
- [69] M. Fukuma, N. Matsumoto, and N. Umeda,
“Implementation of the HMC algorithm on the
tempered Lefschetz thimble method,”
arXiv:1912.13303 [hep-lat].
- [70] H. Fujii, S. Kamata, and Y. Kikukawa, “Monte Carlo
study of Lefschetz thimble structure in one-dimensional
Thirring model at finite density,” *J. High Energ. Phys.*
2016 no. 9, (Sept., 2016) 172.
<http://arxiv.org/abs/1509.09141>. arXiv: 1509.09141.
- [71] C. Itzykson, R. Pearson, and J. Zuber, “Distribution of
zeros in Ising and gauge models,” *Nuclear Physics B*
220 no. 4, (Sept., 1983) 415–433. [https://linkinghub.
elsevier.com/retrieve/pii/0550321383904996](https://linkinghub.elsevier.com/retrieve/pii/0550321383904996).
- [72] C. Pisani and E. R. Smith, “Lee-Yang zeros and stokes
phenomenon in a model with a wetting transition,”
Journal of Statistical Physics **72** no. 1-2, (July, 1993)
51–78.
<http://link.springer.com/10.1007/BF01048040>.